An Overview of Fractal Antenna Engineering Research

Douglas H. Werner[1] and Suman Ganguly[2]

[1]Communications and Space Sciences Laboratory, Department of Electrical Engineering
The Pennsylvania State University, University Park, PA 16802 USA
Tel: +1 (814) 863-2946; E-mail: dhw@psu.edu

[2]Center For Remote Sensing, Inc.
11350 Random Hills Rd., Suite 710, Fairfax, VA 22030 USA
Tel: +1 (703) 385-7717; E-mail: remote703@aol.com

Abstract

Recent efforts by several researchers around the world to combine fractal geometry with electromagnetic theory have led to a plethora of new and innovative antenna designs. In this report, we provide a comprehensive overview of recent developments in the rapidly growing field of fractal antenna engineering. Fractal antenna engineering research has been primarily focused in two areas: the first deals with the analysis and design of fractal antenna elements, and the second concerns the application of fractal concepts to the design of antenna arrays. Fractals have no characteristic size, and are generally composed of many copies of themselves at different scales. These unique properties of fractals have been exploited in order to develop a new class of antenna-element designs that are multi-band and/or compact in size. On the other hand, fractal arrays are a subset of thinned arrays, and have been shown to possess several highly desirable properties, including multi-band performance, low sidelobe levels, and the ability to develop rapid beamforming algorithms based on the recursive nature of fractals. Fractal elements and arrays are also ideal candidates for use in reconfigurable systems. Finally, we will provide a brief summary of recent work in the related area of fractal frequency-selective surfaces.

Keywords: Fractals; electrodynamics; antennas; antenna theory; antenna arrays; frequency selective surfaces; multi-band antennas; log periodic antennas; miniature antennas; antenna radiation patterns

1. Introduction

There has been an ever-growing demand, in both the military as well as the commercial sectors, for antenna designs that possess the following highly desirable attributes:

1. Compact size
2. Low profile
3. Conformal
4. Multi-band or broadband

There are a variety of approaches that have been developed over the years, which can be utilized to achieve one or more of these design objectives. For instance, an excellent overview of various useful techniques for designing compact (i.e., miniature) antennas may be found in [1] and [2]. Moreover, a number of approaches for designing multi-band (primarily, dual-band) antennas have been summarized in [3]. Recently, the possibility of developing antenna designs that exploit in some way the properties of fractals to achieve these goals, at least in part, has attracted a lot of attention.

The term *fractal*, which means broken or irregular fragments, was originally coined by Mandelbrot [4] to describe a family of complex shapes that possess an inherent self-similarity or self-affinity in their geometrical structure. The original inspiration for the development of fractal geometry came largely from an in-depth study of the patterns of nature. For instance, fractals have been successfully used to model such complex natural objects as galaxies, cloud boundaries, mountain ranges, coastlines, snowflakes, trees, leaves, ferns, and much more. Since the pioneering work of Mandelbrot and others, a wide variety of applications for fractals continue to be found in many branches of science and engineering. One such area is *fractal electrodynamics* [5-11], in which fractal geometry is combined with electromagnetic theory for the purpose of investigating a new class of radiation, propagation, and scattering problems. One of the most promising areas of fractal-electrodynamics research is in its application to antenna theory and design.

Traditional approaches to the analysis and design of antenna systems have their foundation in Euclidean geometry. There has been a considerable amount of recent interest, however, in the possibility of developing new types of antennas that employ fractal rather than Euclidean geometric concepts in their design. We refer to this new and rapidly growing field of research as *fractal antenna engineering*. Because fractal geometry is an extension of classical geometry, its recent introduction provides engineers with the unprecedented opportunity to explore a virtually limitless number of previously unavailable configurations for possible use in the development of new and innovative antenna designs. There

are primarily two active areas of research in fractal antenna engineering. These include: 1.) the study of fractal-shaped antenna elements, and 2.) the use of fractals in the design of antenna arrays. The purpose of this article is to provide an overview of recent developments in the theory and design of fractal antenna elements, as well as fractal antenna arrays. The related area of fractal frequency-selective surfaces will also be considered in this article.

We note that there are a number of patents on fractal antenna designs that have been filed and awarded in recent years. The purpose of this article, however, is to present an overview of letters and papers published in technical journals that deal with the subject of fractal antenna engineering. Therefore, the contents of specific patents will not be discussed here. The interested reader is encouraged to search the various patent databases for this information.

2. Some Useful Geometries for Fractal Antenna Engineering

This section will present a brief overview of some of the more common fractal geometries that have been found to be useful in developing new and innovative designs for antennas. The first fractal that will be considered is the popular Sierpinski gasket [12]. The first few stages in the construction of the Sierpinski gasket are shown in Figure 1. The procedure for geometrically constructing this fractal begins with an equilateral triangle contained in the plane, as illustrated in Stage 0 of Figure 1. The next step in the construction process (see Stage 1 of Figure 1) is to remove the central triangle with vertices that are located at the midpoints of
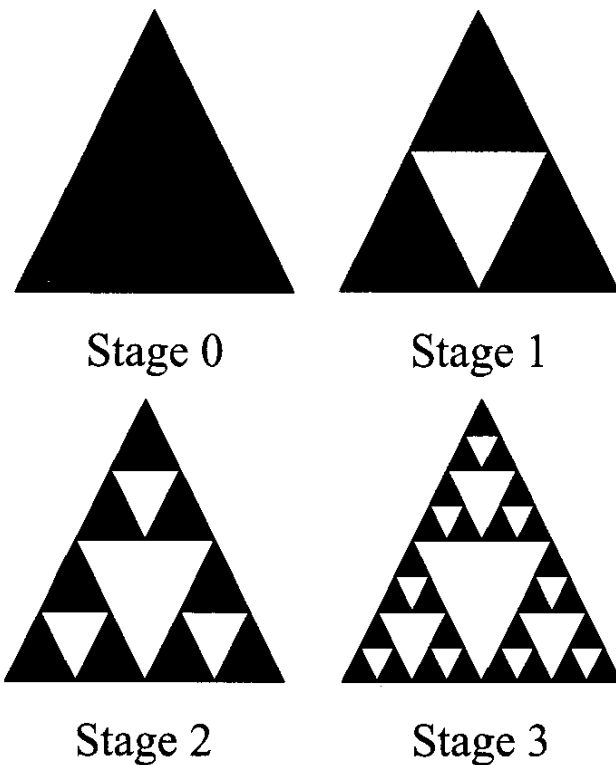

Stage 0   Stage 1

Stage 2   Stage 3

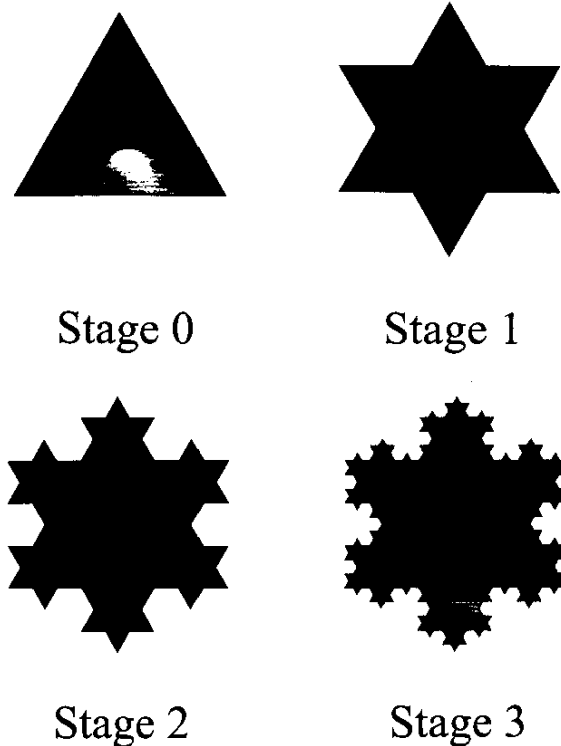**Figure 2. The first few stages in the construction of a Koch snowflake.**

Figure 3. A Stage 4 ternary fractal tree.

Stage 0   Stage 1

Stage 2   Stage 3

Figure 1. Several stages in the construction of a Sierpinski gasket fractal.
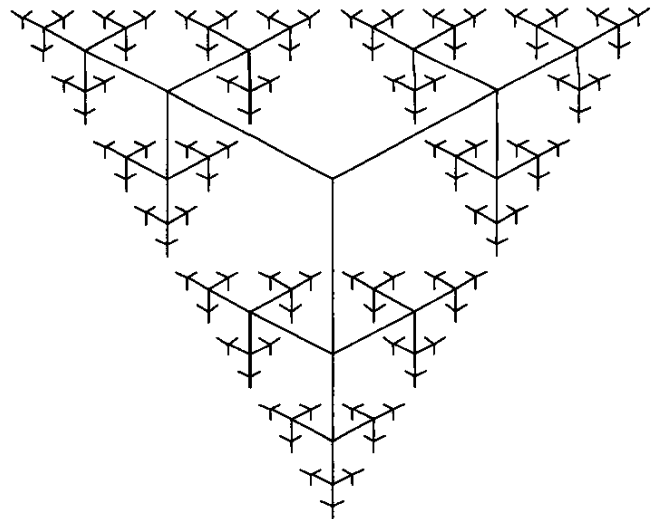
the sides of the original triangle, shown in Stage 0. This process is then repeated for the three remaining triangles, as illustrated in Stage 2 of Figure 1. The next two stages (i.e., Stages 3 and 4) in the construction of the Sierpinski gasket are also shown in Figure 1. The Sierpinski-gasket fractal is generated by carrying out this iterative process an infinite number of times. It is easy to see from this definition that the Sierpinski gasket is an example of a self-similar fractal. From an antenna engineering point of view, a useful interpretation of Figure 1 is that the black triangular areas represent a metallic conductor, whereas the white triangular areas represent regions where metal has been removed.

Another popular fractal is known as the Koch snowflake [12]. This fractal also starts out as a solid equilateral triangle in the plane, as illustrated in Stage 0 of Figure 2. However, unlike the Sierpinski gasket, which was formed by systematically removing smaller and smaller triangles from the original structure, the Koch snowflake is constructed by adding smaller and smaller triangles to the structure in an iterative fashion. This process is clearly represented in Figure 2, where the first few stages in the geometrical construction of a Koch snowflake are shown.

A number of structures based on purely deterministic or random fractal trees have also proven to be extremely useful in developing new design methodologies for antennas and frequency-selective surfaces. An example of a deterministic ternary (three-branch) fractal tree is shown in Figure 3. This particular ternary-tree structure is closely related to the Sierpinski gasket shown in Figure 1. In fact, the ternary-tree geometry illustrated in Figure 3 can be interpreted as a wire equivalent model of the Stage 4 Sierpinski gasket shown in Figure 1.

The space-filling properties of the Hilbert curve and related curves make them attractive candidates for use in the design of fractal antennas. The first four steps in the construction of the Hilbert curve are shown in Figure 4 [12]. The Hilbert curve is an example of a space-filling fractal curve that is self-avoiding (i.e., has no intersection points).

Some of the more common fractal geometries that have found applications in antenna engineering are depicted in Figure 5. The Koch snowflakes and islands have been primarily used to
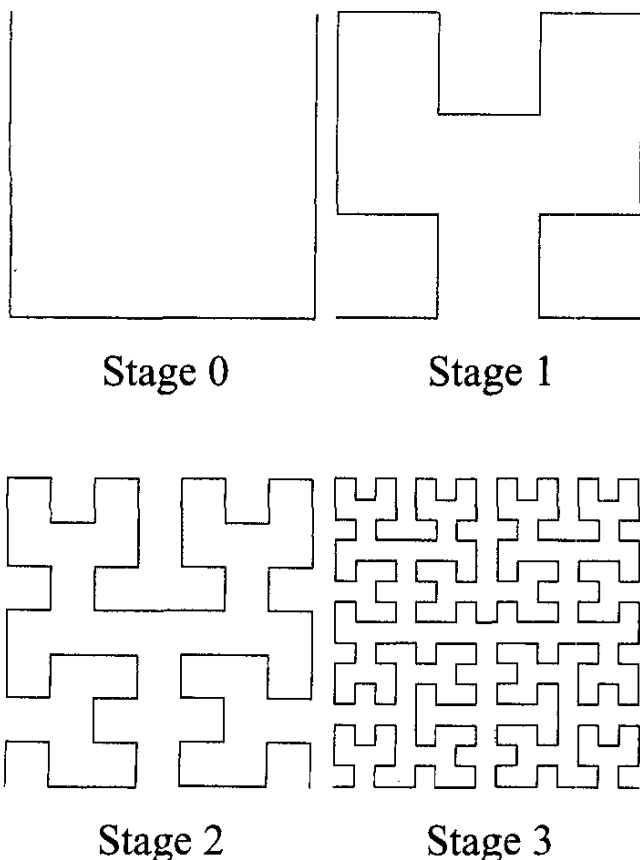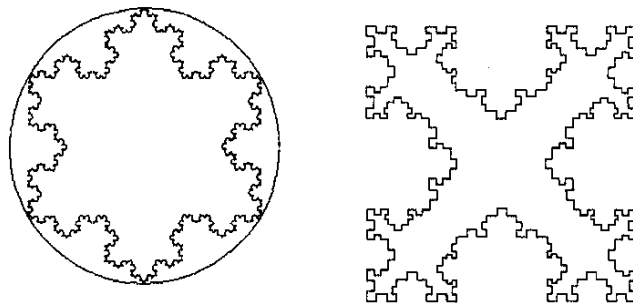

Figure 5a. Some common fractal geometries found in antenna applications: Koch snowflakes/islands. These are used in miniaturized loop antennas and miniaturized patch antennas.
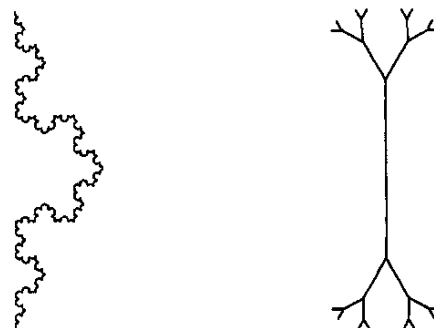

Figure 5b. Some common fractal geometries found in antenna applications: Koch curves and fractal trees, used in miniaturized dipole antennas.
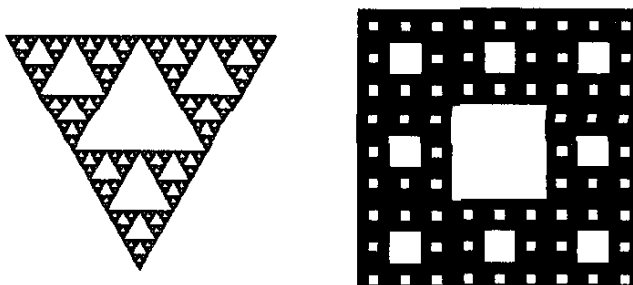

Figure 5c. Some common fractal geometries found in antenna applications: Sierpinski gaskets and carpets, used in multi-band antennas.

develop new designs for miniaturized-loop as well as microstrip-patch antennas. New designs for miniaturized dipole antennas have also been developed based on a variety of Koch curves and fractal trees. Finally, the self-similar structure of Sierpinski gaskets and carpets has been exploited to develop multi-band antenna elements.

3. Iterated Function Systems: The Language of Fractals

Iterated function systems (IFS) represent an extremely versatile method for conveniently generating a wide variety of useful

Stage 0   Stage 1

Stage 2   Stage 3

Figure 4. The first few stages in the construction of a Hilbert curve.

fractal structures [12, 13]. These iterated function systems are based on the application of a series of affine transformations, w, defined by

$$w\begin{pmatrix} x \\ y \end{pmatrix} = \begin{pmatrix} a & b \\ c & d \end{pmatrix}\begin{pmatrix} x \\ y \end{pmatrix} + \begin{pmatrix} e \\ f \end{pmatrix}, \qquad (1)$$

or, equivalently, by

$$w(x, y) = (ax + by + e, cx + dy + f), \qquad (2)$$

where a, b, c, d, e, and f are real numbers. Hence, the affine transformation, w, is represented by six parameters

$$\begin{pmatrix} a & b & | & e \\ c & d & | & f \end{pmatrix}, \qquad (3)$$

such that a, b, c, and d control rotation and scaling, while e and f control linear translation.

Now suppose we consider w_1, w_2, $\cdots$, w_N as a set of affine linear transformations, and let A be the initial geometry. Then a new geometry, produced by applying the set of transformations to the original geometry, A, and collecting the results from $w_1(A)$, $w_2(A)$, $\cdots$, $w_N(A)$, can be represented by

$$W(A) = \bigcup_{n=1}^{N} w_n(A), \qquad (4)$$

where W is known as the Hutchinson operator [12]. A fractal geometry can be obtained by repeatedly applying W to the previous geometry. For example, if the set A_0 represents the initial geometry, then we will have

$$A_1 = W(A_0), \quad A_2 = W(A_1), \quad \cdots, \quad A_{k+1} = W(A_k). \qquad (5)$$

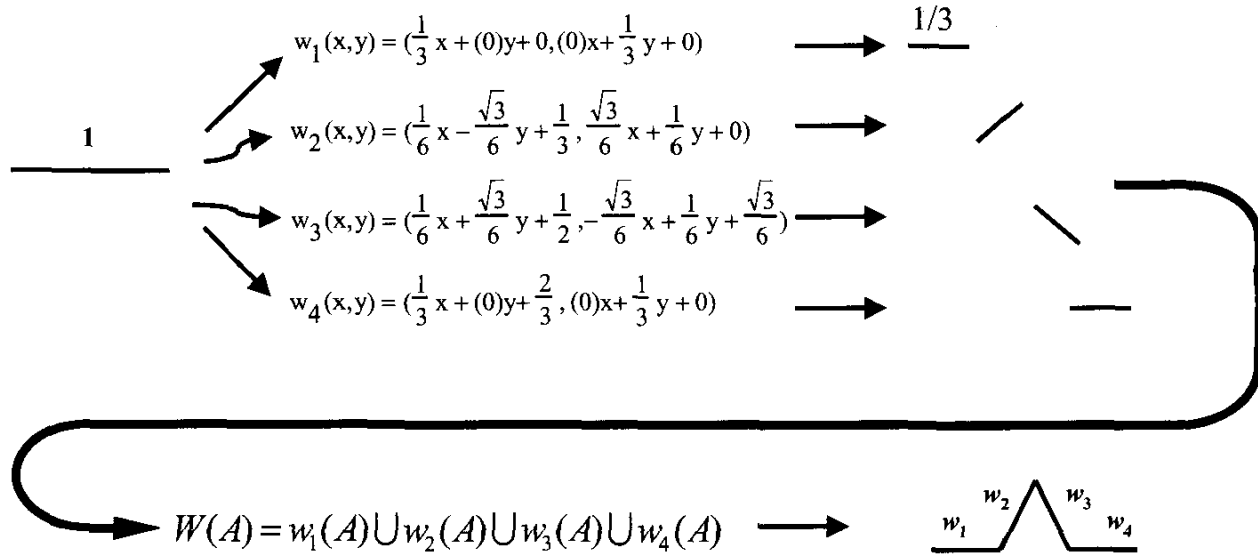An iterated function system generates a sequence that converges to a final image, A_∞, in such a way that

$$w_1(x,y) = (\frac{1}{3}x + (0)y + 0, (0)x + \frac{1}{3}y + 0)$$

$$w_2(x,y) = (\frac{1}{6}x - \frac{\sqrt{3}}{6}y + \frac{1}{3}, \frac{\sqrt{3}}{6}x + \frac{1}{6}y + 0)$$

$$w_3(x,y) = (\frac{1}{6}x + \frac{\sqrt{3}}{6}y + \frac{1}{2}, -\frac{\sqrt{3}}{6}x + \frac{1}{6}y + \frac{\sqrt{3}}{6})$$

$$w_4(x,y) = (\frac{1}{3}x + (0)y + \frac{2}{3}, (0)x + \frac{1}{3}y + 0)$$

$$W(A) = w_1(A) \bigcup w_2(A) \bigcup w_3(A) \bigcup w_4(A)$$

Figure 6. The standard Koch curve as an iterated function system (IFS).

Iteration 1   Iteration 2   Iteration 3
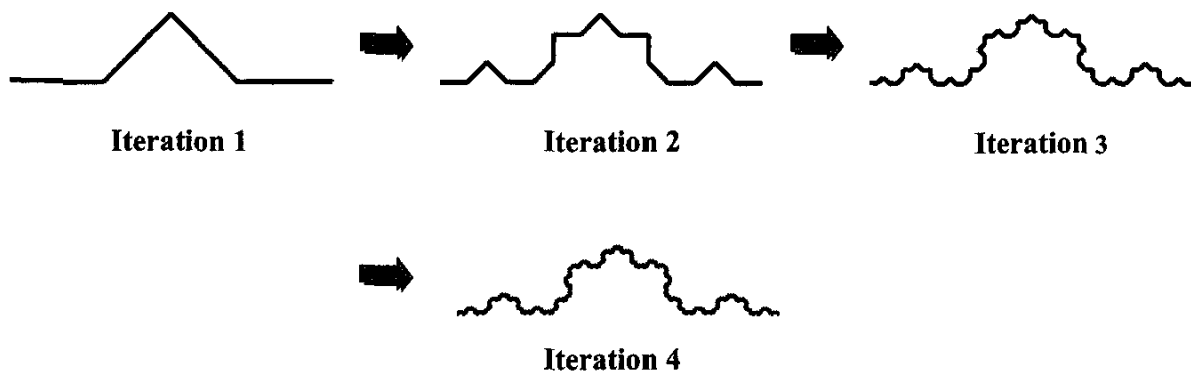
Iteration 4

Figure 7. The first four stages in the construction of the standard Koch curve via an iterated function system (IFS) approach. The transformation is applied for each iteration to achieve higher levels of fractalization.

$$W(A_\infty) = A_\infty. \tag{6}$$

This image is called the attractor of the iterated function system, and represents a "fixed point" of W.

Figure 6 illustrates the iterated function system procedure for generating the well-known Koch fractal curve. In this case, the initial set, A_0, is the line interval of unit length, i.e., $A_0 = \{x : x \in [0,1]\}$. Four affine linear transformations are then applied to A_0, as indicated in Figure 6. Next, the results of these four linear transformations are combined together to form the first iteration of the Koch curve, denoted by A_1. The second iteration of the Koch curve, A_2, may then be obtained by applying the same four affine transformations to A_1. Higher-order versions of the Koch curve are generated by simply repeating the iterative process until the desired resolution is achieved. The first four iterations of the Koch curve are shown in Figure 7. We note that these curves would converge to the actual Koch fractal, represented by A_∞, as the number of iterations approaches infinity.

Iterated function systems have proven to be a very powerful design tool for fractal antenna engineers. This is primarily because they provide a general framework for the description, classification, and manipulation of fractals [13]. In order to further illustrate this important point, the iterated function system code for such diverse objects as a Sierpinski gasket and a fractal tree have been provided in Figure 8 and Figure 9, respectively [12].

a	b	c	d	e	f
0.195	-0.488	0.344	0.443	0.4431	0.2452
0.462	0.414	-0.252	0.361	0.2511	0.5692
-0.058	-0.07	0.453	-0.111	0.5976	0.0969
-0.035	0.07	-0.469	-0.022	0.4884	0.5069
-0.637	0.0	0.0	0.501	0.8562	0.2513

Figure 9. The iterated function system code for a fractal tree.

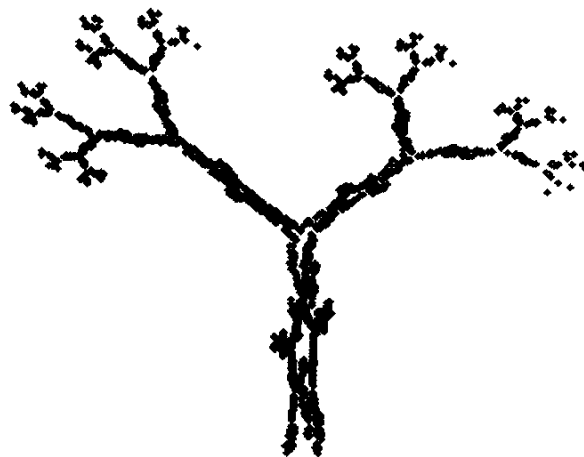| a	b	c	d	e	f
0.500	0.000	0.000	0.500	0.000	0.000
0.500	0.000	0.000	0.500	0.500	0.000
0.500	0.000	0.000	0.500	0.000	0.500

Figure 8. The iterated function system code for a Sierpinski gasket.

4. Fractal Antenna Elements

4.1 Early Work on Fractal Loop, Dipole, and Monopole Antennas

Apparently, the earliest published reference to use the terms *fractal radiators* and *fractal antennas* to denote fractal-shaped antenna elements appeared in May, 1994 [14]. Prior to this, the terminology had been introduced publicly during an invited IEEE seminar held at Bucknell University in November, 1993 [15]. The application of fractal geometry to the design of wire antenna elements was first reported in a series of articles by Cohen [16-19]. These articles introduce the notion of *fractalizing* the geometry of a standard dipole or loop antenna. This is accomplished by systematically bending the wire in a fractal way, so that the overall arc length remains the same, but the size is correspondingly reduced with the addition of each successive iteration. It has been demonstrated that this approach, if implemented properly, can lead to efficient miniaturized antenna designs. For instance, the radiation characteristics of Minkowski dipoles and Minkowski loops were originally investigated in [16-19]. Properties of the Koch fractal monopole were later considered in [20, 21]. It was shown that the electrical performance of Koch fractal monopoles is superior to that of conventional straight-wire monopoles, especially when operated in the small-antenna frequency regime. A fast approximation technique for evaluating the radiation characteristics of the Koch fractal dipole was presented in [22]. Monopole configurations with fractal top-loads have also been considered in [23, 24],
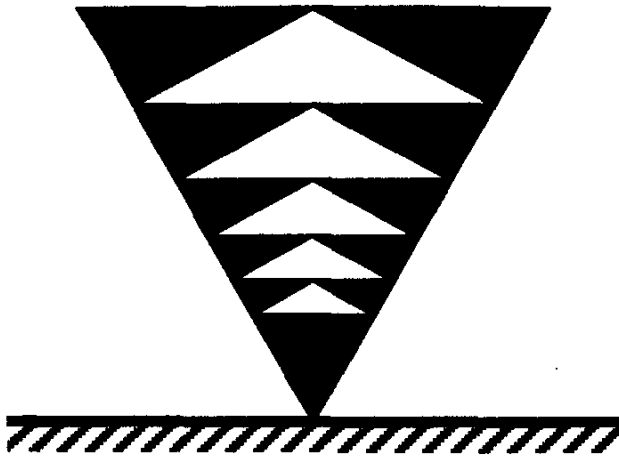
Figure 10a. Variations of the Sierpinski gasket and related multi-band monopole antennas: a multi-triangular monopole
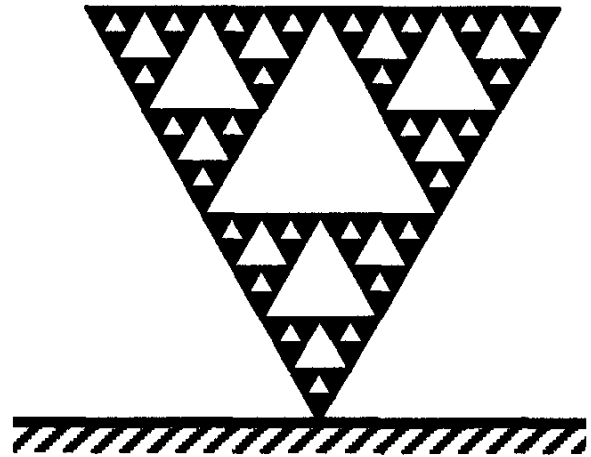

Figure 10b. Variations of the Sierpinski gasket and related multi-band monopole antennas: a standard Sierpinski monopole with $\alpha = 60°$ and $\delta = 2$.
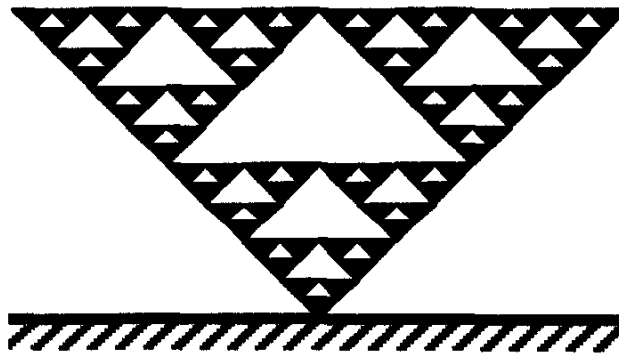

Figure 10c. Variations of the Sierpinski gasket and related multi-band monopole antennas: a Sierpinski monopole with $\alpha = 90°$ and $\delta = 2$.
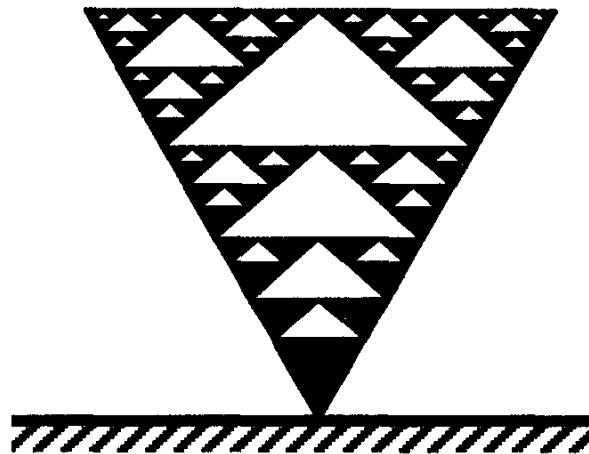

Figure 10d. Variations of the Sierpinski gasket and related multi-band monopole antennas: a Sierpinski monopole with $\alpha = 60°$ and $\delta = 1.5$.
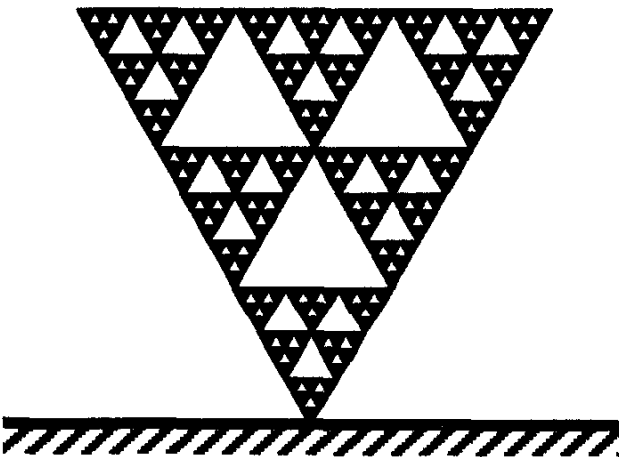

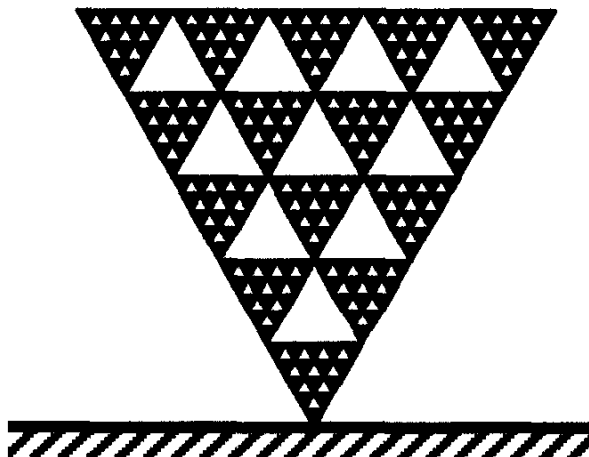Figure 10e. Variations of the Sierpinski gasket and related multi-band monopole antennas: a mod-3 Sierpinski monopole.

Figure 10f. Variations of the Sierpinski gasket and related multi-band monopole antennas: a mod-5 Sierpinski monopole.
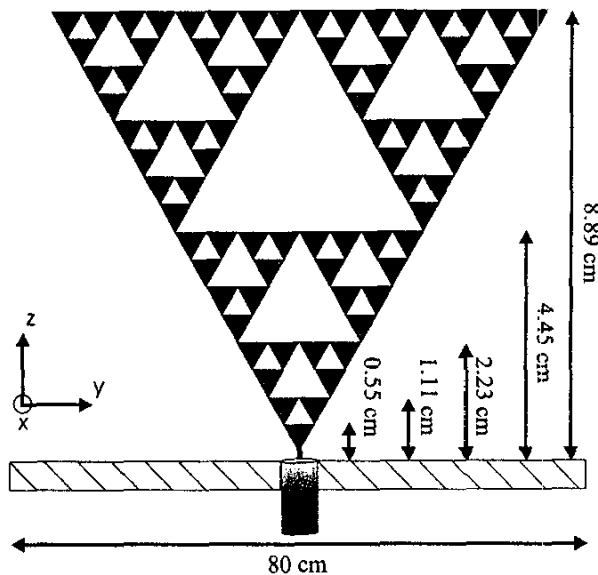
as an alternative technique for achieving size miniaturization. Finally, the effects of various types of symmetries on the performance of Koch dipole antennas were studied by Cohen [25, 26].

4.2 Research on Sierpinski Gasket Antennas

A multi-band fractal monopole antenna, based on the Sierpinski gasket, was first introduced by Puente et al. [27, 28]. The original Sierpinski monopole antenna is illustrated in Figure 10b. In this case, the antenna geometry is in the form of a classical Sierpinski gasket, with a flare angle of $\alpha = 60°$ and a self-similarity scale factor of $\delta = 2$. The dimensions for a prototype Sierpinski gasket monopole are given in Figure 11. Figure 11 also contains plots of simulated and measured values of the input reflection coefficient versus frequency for the antenna, along with the associated curves for input resistance and reactance. A scheme for modifying the spacing between the bands of the Sierpinski monopole was subsequently presented in [29], and later summarized in [11]. Figure 10d shows an example of a Sierpinski monopole antenna with a flare angle of $\alpha = 60°$ and a self-similarity scale factor of $\delta = 1.5$. It was demonstrated in [29] that the positions of the multiple bands may be controlled by proper adjustment of the scale factor used to generate the Sierpinski antenna. The transient response of the multi-band Sierpinski monopole was investigated in [30]. This was accomplished by using a Method of Moments technique to solve the time-domain electric-field integral equation via a marching-on-in-time procedure. Linear parametric modeling techniques were also applied, in order to considerably reduce computation time. The dependence of the radiation characteristics of the Sierpinski monopole on flare angle was documented in [31]. Figure 10c shows an example of a Sierpinski monopole with a flare angle of $\alpha = 90°$ and a self-similarity scale factor of $\delta = 2$. Further investigations concerning enhancing the performance of Sierpinski-gasket monopoles through perturbations in their geometry were reported in [32]. It was found that a variation in the flare angle of the antenna translated into a shift of the operating bands, as well as into a change in the input impedance and radiation patterns. Fast iterative network models that are useful for predicting the performance of Sierpinski fractal antennas were developed in [33-35]. The predicted self-similar surface-current distribution on a Sierpinski monopole antenna was verified in [36, 37] by using infra-red thermograms. Breden and Langley [38] presented measurements of input impedance and radiation patterns for several printed fractal antennas, including Koch and Sierpinski monopoles.

4.3 Research on Fractal Tree Antennas

The multi-band characteristics of a deterministic fractal tree structure were considered in [39]. On the other hand, the multi-band properties of random fractal tree-like antennas, created by an electrochemical deposition process, were investigated by Puente et al. [40]. It was found that these fractal tree antennas have a multi-band behavior with a denser band distribution than the Sierpinski antenna. The multi-band and wide-band properties of printed fractal branched antennas were studied in [41]. Werner et al. [42] considered the multi-band electromagnetic properties of thin-wire structures based on a ternary-tree fractal geometry. In particular, the impedance behavior of a tri-band ternary fractal tree was studied by carrying out a numerically rigorous Method of Moments

Figure 11a. A five-iteration Sierpinski monopole, showing the dimensions [11].
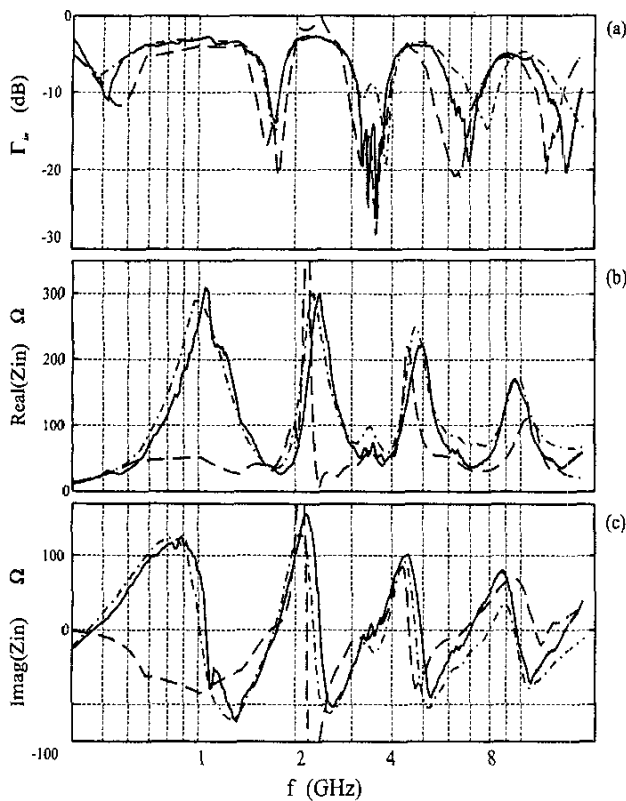
8.89 cm
4.45 cm
2.23 cm
1.11 cm
0.55 cm
80 cm

Figure 11b. The input reflection coefficient, Γ_{in}, relative to 50 Ω (a); the input resistance, R_{in} (b); and the input reactance X_{in} (c) of a the five-iteration Sierpinski monopole of Figure 11a [11]. The experimental data are the solid curves, an FDTD calculation is the dashed curves, and _DOTIG4_ was used to compute the dashed-dotted curves.

Γ_{in} (dB)
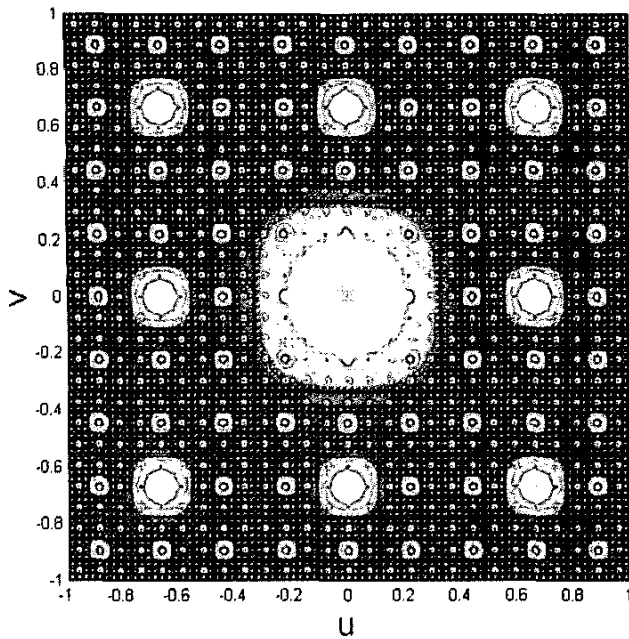Real(Zin) Ω
Imag(Zin) Ω
f (GHz)

Figure 17. A contour plot showing the self-similar fractal structure of the far-field radiation pattern of a multi-band Weierstrass planar array, with $P = 5$ and $\gamma = 0.5$.
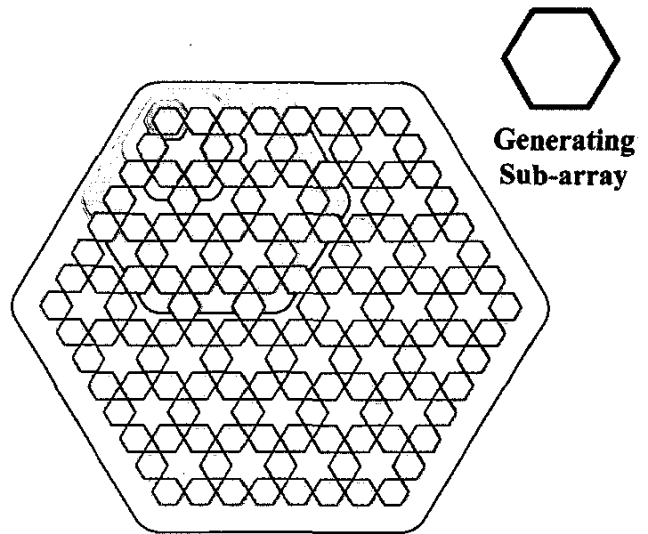

Figure 18. A schematic representation for a recursively generated thinned hexagonal array. The first four stages of growth are indicated by the blue (Stage 1), red (Stage 2), green (Stage 3), and orange (Stage 4) arrays respectively. The six-element generating sub-array is shown in the upper-right-hand corner, where the elements are located at the vertices of the hexagon.
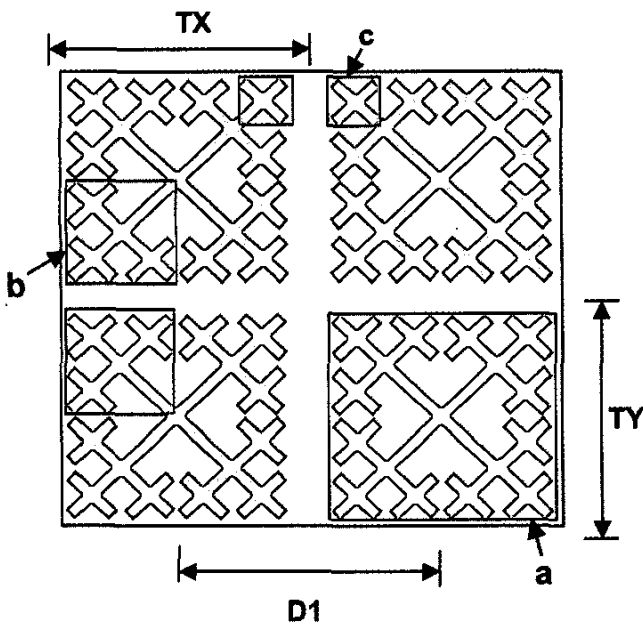

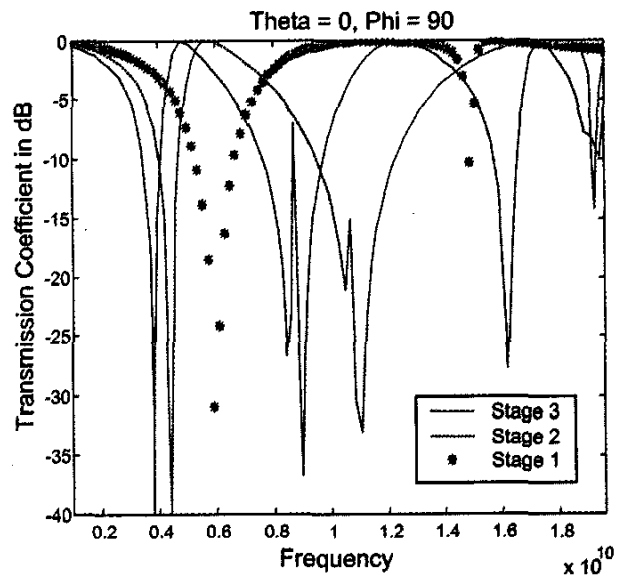Figure 23a. A tri-band FSS design based on the crossbar fractal tree structure shown in Figure 22.

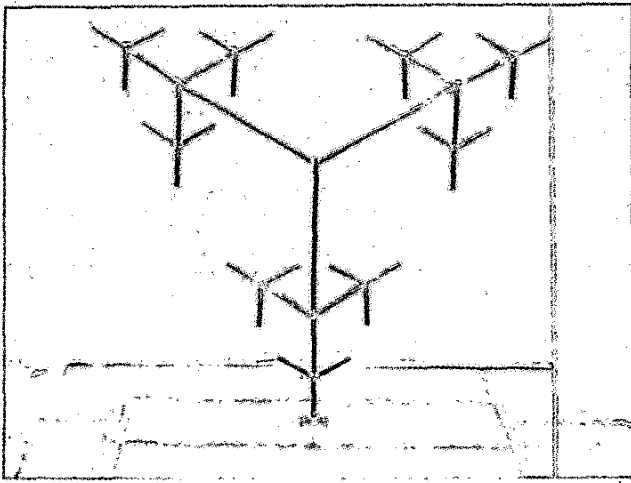Figure 23b. The transmission coefficient for the FSS of Figure 23a.

Figure 12. A photograph of a prototype tri-band ternary fractal tree antenna.

analysis of the structure. The unique multi-band properties of the antenna were confirmed by comparing the results of the numerical simulations with actual measurements. A photograph of the prototype tri-band ternary fractal tree antenna, which was constructed and measured, is shown in Figure 12. The space-filling properties of two-dimensional and three-dimensional fractal trees were suggested by Gianvittorio and Rahmat-Samii [43, 44] as good candidates for application to the design of miniaturized antennas. It was shown that a reduction in the resonant frequency of a standard dipole can be achieved by end-loading it with two-dimensional or three-dimensional tree-like fractal structures. This decrease in resonant frequency was shown to asymptotically approach a limit as the number of iterations are increased. Ways to improve antenna-miniaturization techniques were discussed in [45], employing fractal tree geometries as end-loads by increasing the density of branches (i.e., by using trees with a higher fractal dimension).

4.4 Fractal Volume Antennas

The concept of a fractal volume antenna was introduced in [46], and was demonstrated as a means of increasing the degrees of design freedom for planar fractal antennas, at the expense of some small increase in antenna thickness. Some examples of fractal volume antennas were presented, including a triangular Sierpinski carpet monopole, and a square Sierpinski carpet microstrip antenna. A novel design for a wide-band fractal monopole antenna that used stacked square and diamond Sierpinski carpets was introduced in [47]. The design was shown to essentially achieve a good input impedance match throughout a 1-20 GHz pass band. Other examples of fractal volume antennas include the stacked Sierpinski monopole, considered in [48], and the stacked Sierpinski microstrip patch, considered in [49]. The latter approach made use of small parasitically coupled fractal patch elements, in order to increase the bandwidth compared to a single active fractal patch antenna.

4.5 Variations of Sierpinski Gasket Antennas and the Hilbert Curve Antenna

Dual-band designs, based on a variation of the Sierpinski fractal monopole, were presented in [50] and [51]. Specific applications of these designs to emerging GSM and DECT technologies were discussed. The multi-band properties of fractal monopoles based on the generalized family of mod-p Sierpinski gaskets were recently investigated by Castany et al. [52]. The advantage of this approach is that it provides a high degree of flexibility in choosing the number of bands and the associated band spacings for a candidate antenna design. Examples of a mod-3 and a mod-5 Sierpinski monopole are shown in Figure 10e and Figure 10f, respectively. A novel configuration of a shorted fractal Sierpinski gasket antenna was presented and discussed in [53]. Figure 10a shows a multi-triangular monopole antenna, which is a variation of the Parany antenna, originally considered in [54]. These multi-triangular antennas have been shown to exhibit multi-band properties with respect to input impedance and radiation patterns, even though their geometry is not strictly fractal. In particular, the properties of the Parany antenna are very similar to those of the Sierpinski antenna shown in Figure 10b. An approach for designing short dual-band multi-triangular monopole antennas was reported in [55]. This approach has the highly-desirable feature of a band ratio of less that two between the first and second bands.

The space-filling properties of the Hilbert curve were investigated in [56] and [57] as an effective method for designing compact resonant antennas. The effect of the feed-point location on the input impedance of a Hilbert curve antenna was studied in [58]. It
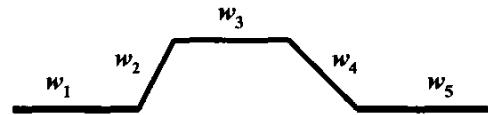
$$w_1(x,y) = (a_1x + b_1y + e_1, c_1x + d_1y + f_1)$$

$$w_2(x,y) = (a_2x + b_2y + e_2, c_2x + d_2y + f_2)$$

$$w_3(x,y) = (a_3x + b_3y + e_3, c_3x + d_3y + f_3)$$

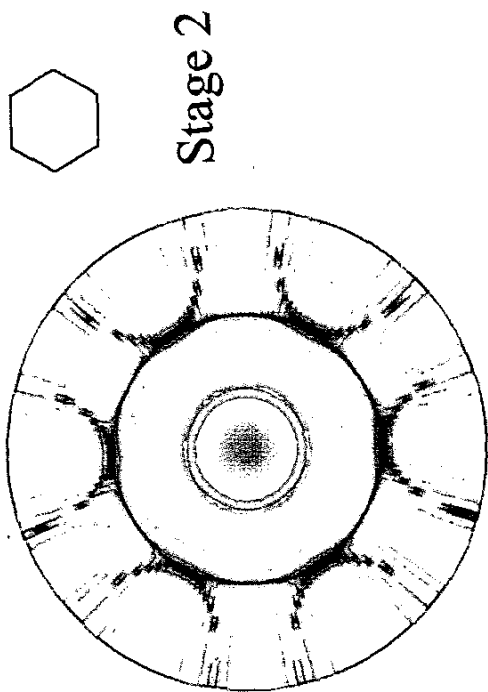$$w_4(x,y) = (a_4x + b_4y + e_4, c_4x + d_4y + f_4)$$

$$w_5(x,y) = (a_5x + b_5y + e_5, c_5x + d_5y + f_5)$$

$$W(x,y) = w_1(x,y) \cup w_2(x,y) \cup w_3(x,y) \cup w_4(x,y) \cup w_5(x,y)$$
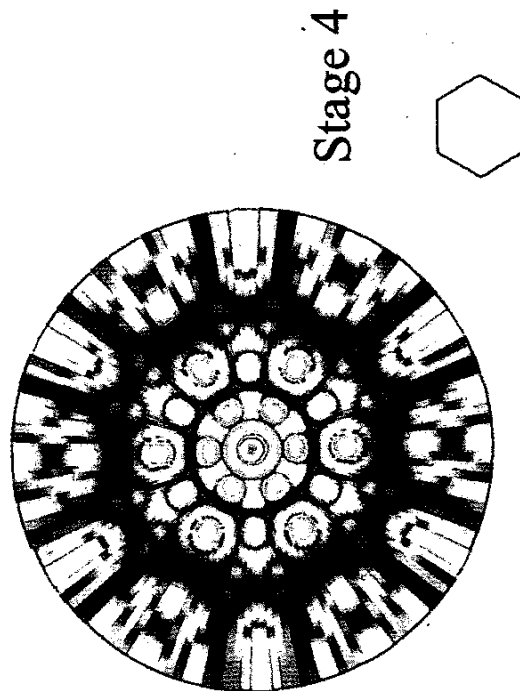
where a_n, b_n, c_n, d_n, e_n, f_n are the parameters to be selected by the GA.

Figure 13. The generator and associated iterated function system (IFS) code for fractal dipole antennas of arbitrary shape.

Stage 2

Figure 19b. A contour plot of the radiation pattern for Stage 2 of the recursively generated thinned hexagonal arrays shown in Figure 18.

Stage 4

Figure 19d. A contour plot of the radiation pattern for Stage 4 of the recursively generated thinned hexagonal arrays shown in Figure 18.
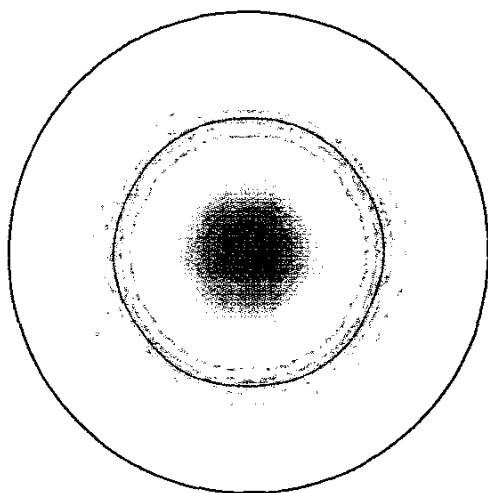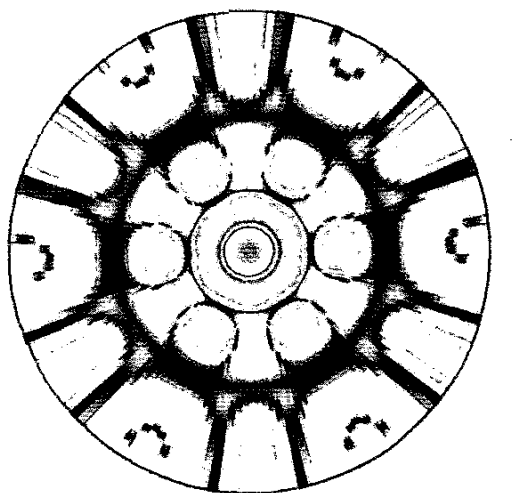
Stage 1

Figure 19a. A contour plot of the radiation pattern for Stage 1 of the recursively generated thinned hexagonal arrays shown in Figure 18.

Stage 3

Figure 19c. A contour plot of the radiation pattern for Stage 3 of the recursively generated thinned hexagonal arrays shown in Figure 18.
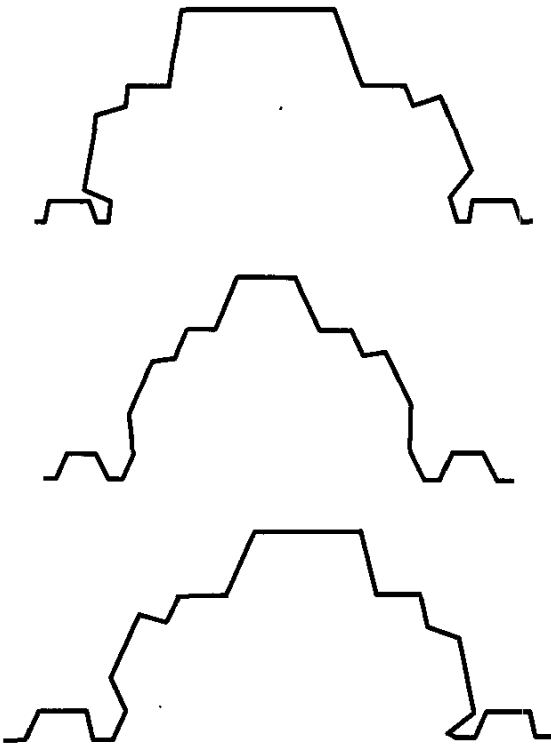
Figure 14. Some examples of genetically engineered fractal dipole antennas.

was shown that while a center-fed Hilbert curve antenna may result in a very small radiation resistance, a properly chosen off-center feed point can always provide a 50Ω match, regardless of the stage of growth.

4.6 Research on Fractal Patch Antennas

Borja and Romeu [59] proposed a design methodology for a multi-band Sierpinski microstrip patch antenna. A technique was introduced to improve the multi-band behavior of the radiation patterns by suppressing the effects of high-order modes. Finally, high-directivity modes in a Koch-island fractal patch antenna were studied in [60, 61]. It was shown that a patch antenna with a Koch fractal boundary exhibits localized modes at a certain frequency above the fundamental mode, which can lead to broadside directive patterns. Localized modes were also observed in a waveguide having Koch fractal boundaries [62].

Some additional applications of fractal concepts to the design of microstrip-patch antennas were considered in [63-67]. For instance, [63] introduced a modified Sierpinski-gasket patch antenna for multi-band applications. A design technique for bowtie microstrip-patch antennas, based on the Sierpinski-gasket fractal, was presented in [64]. A computationally efficient Method of Moments formulation was developed in [65], specifically for the analysis of Sierpinski fractal patch antennas. The radiation characteristics of Koch-island fractal microstrip-patch antennas were investigated in [66]. Still other configurations for miniaturized fractal patch antennas were reported by Gianvittorio and Rahmat-Samii [67].

4.7 Combination of Genetic Algorithms with Iterated Function Systems

A powerful design-optimization technique for fractal antennas has been developed by combining genetic algorithms (GA) with iterated function systems (IFS). This GA/IFS technique was successfully used as a design synthesis tool for miniature multi-band fractal antenna elements [68-70]. The fractal antenna element geometries considered in [68-70] were created via an IFS approach by employing an appropriate set of affine transformations, similar to those used in the formulation of the standard Koch curve shown in Figure 6 and Figure 7. The general shape of the generating antenna, along with the appropriate set of affine transformations that constitutes the IFS, are indicated in Figure 13. Figure 14 shows three different examples of genetically engineered Stage 2 fractal dipole antennas. The GA/IFS technique introduced in [68-70] is capable of simultaneously optimizing the fractal antenna geometry, the locations of parallel LC reactive loads on the antenna, and the corresponding component values of these loads.
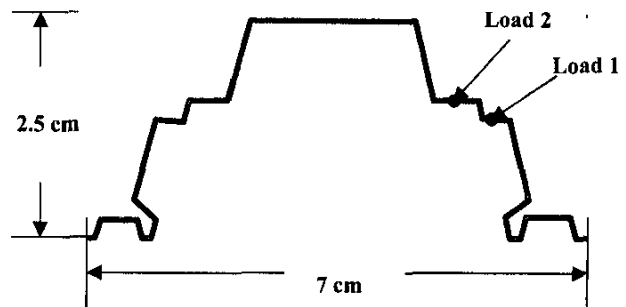
| Load 1: | $C1 = 3.0$ pF $L1 = 2.7$ nH |
| Load 2: | $C2 = 3.3$ pF $L2 = 3.3$ nH |

| VSWR: | 1.33 | at | f = 1225 MHz |
| VSWR: | 1.10 | at | f = 1575 MHz |

Figure 15a. A genetically engineered miniature dual-band fractal dipole antenna element with parallel LC loads.
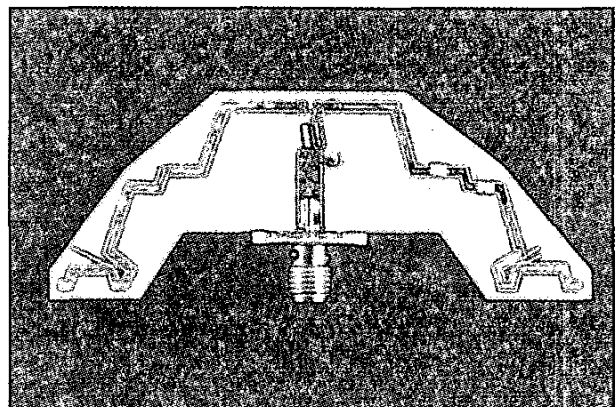
Figure 15b. A photograph of the dual-band fractal dipole antenna in Figure 15a.

Figure 21a. A plot showing the magnitude of the impedance matrix for Stage 1 of the triadic Cantor linear fractal array.

Figure 21d. A plot showing the magnitude of the impedance matrix for Stage 4 of the triadic Cantor linear fractal array.

Figure 21b. A plot showing the magnitude of the impedance matrix for Stage 2 of the triadic Cantor linear fractal array.

Figure 21e. A plot showing the magnitude of the impedance matrix for Stage 5 of the triadic Cantor linear fractal array.
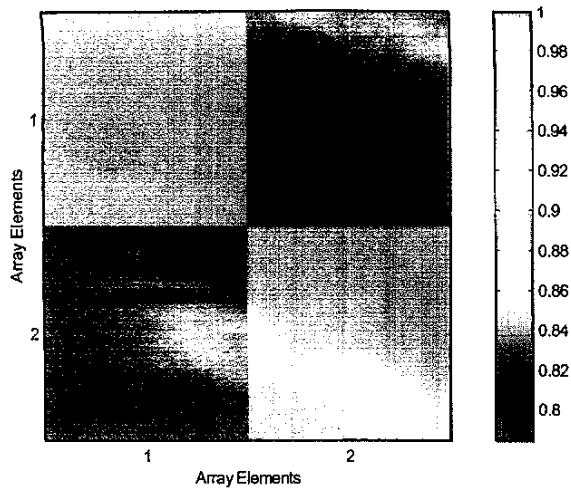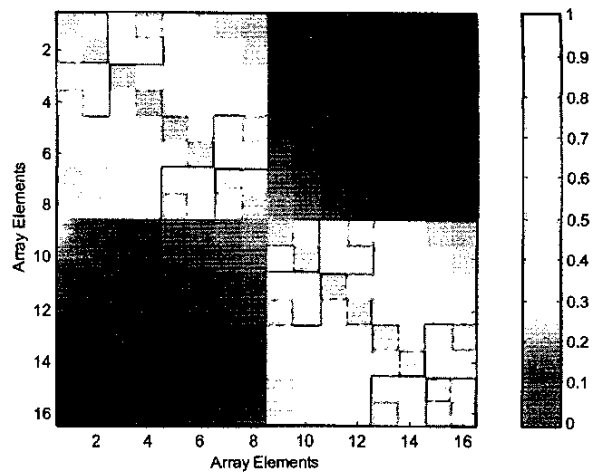

Figure 21c. A plot showing the magnitude of the impedance matrix for Stage 3 of the triadic Cantor linear fractal array.
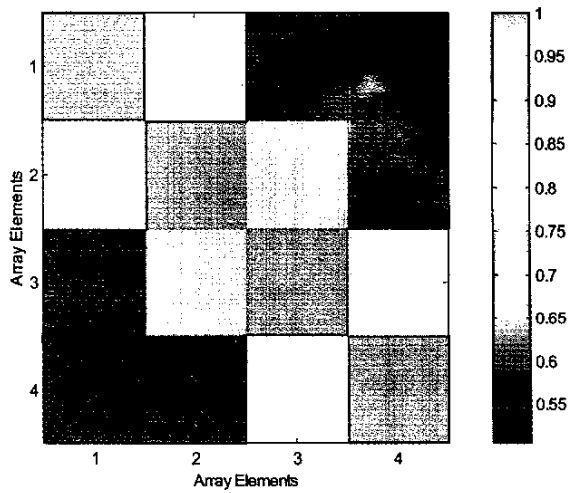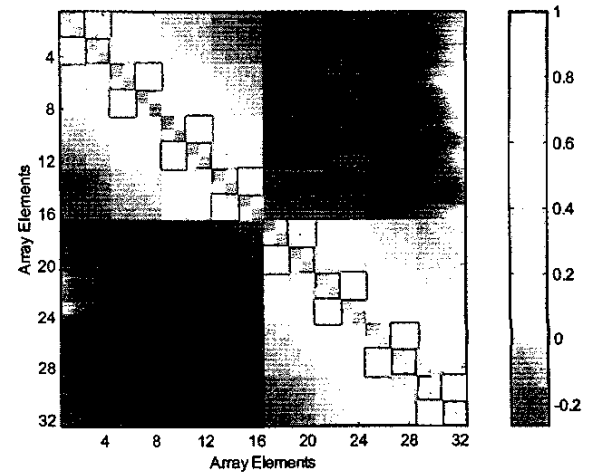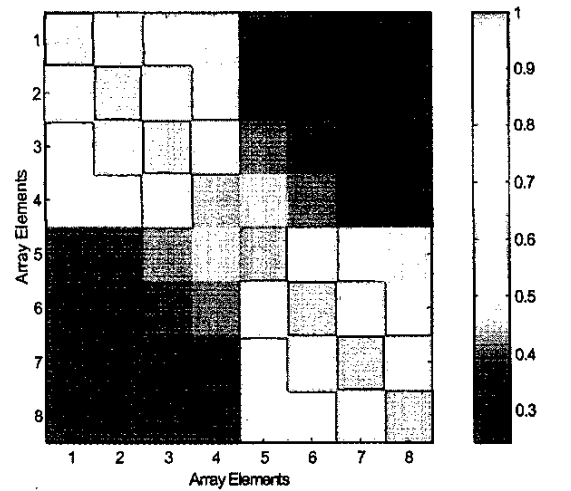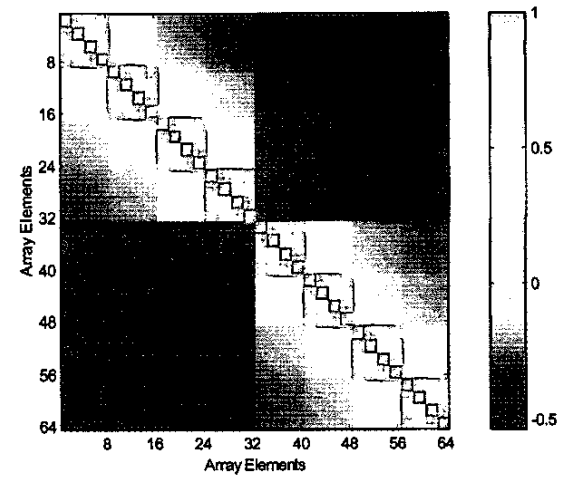

Figure 21f. A plot showing the magnitude of the impedance matrix for Stage 6 of the triadic Cantor linear fractal array.
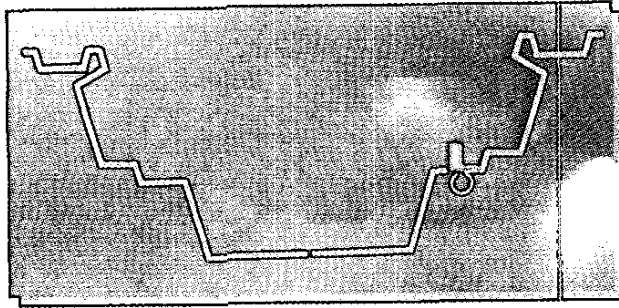
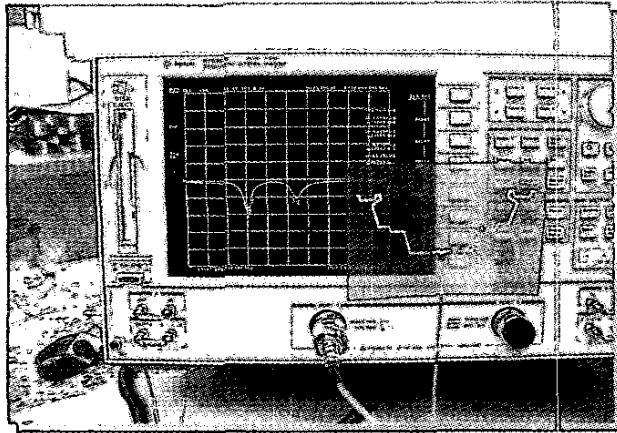Figure 16a. A dual-band direct-write fractal dipole antenna with a direct-write passive LC load on Kapton.

Figure 16b. The measured frequency response (i.e., S_{11} versus frequency) of the antenna in Figure 16a is shown via a network-analyzer screen trace. The vertical axis is 10 dB per division with 0 dB as the reference.

The "fractalization" of the wire antenna allows it to be miniaturized, while the reactive loads are used to achieve multi-band behavior. An example of an optimized multi-band fractal antenna is shown in Figure 15. The objective in this case was to design a miniature dual-band antenna that had a VSWR below 2:1 at $f_1 = 1.575$ GHz and $f_2 = 1.225$ GHz. The geometry of the optimized fractal antenna, together with the required load locations and component values, are provided in Figure 15. A photograph showing a prototype of the fractal antenna is also included in Figure 15. The sensitivity of the radiation characteristics of the genetically engineered miniature multi-band fractal dipole antennas to load component values was considered in [71]. As a consequence of this study, several new optimization approaches were developed, which resulted in antenna designs with considerably reduced load sensitivity. A direct-write process for fabricating miniature reactively loaded fractal dipole antennas was introduced in [72]. The direct-write approach was compared to a traditional board-routed counterpart, incorporating soldered commercial components. A photograph of a miniature loaded dual-band fractal dipole antenna that was direct-written on Kapton is shown in Figure 16. A plot of the measured S_{11} versus frequency for the antenna is also shown in Figure 16 (see the screen trace on the network analyzer). The measured data clearly show the dual-band behavior of the fractal antenna.

5. Fractal Arrays

5.1 Deterministic and Random Fractal Arrays

The term *fractal antenna arrays* was originally coined by Kim and Jaggard in 1986 [73] to denote a geometrical arrangement of antenna elements that is fractal. Properties of random fractals were first used in [73] to develop a design methodology for quasi-random arrays. In other words, random fractals were used to generate array configurations that were somewhere between completely ordered (i.e., periodic) and completely disordered (i.e., random). The main advantage of this technique is that it yields sparse arrays that possess relatively low sidelobes (a feature typically associated with periodic arrays, but not random arrays), and which are also robust (a feature typically associated with random arrays, but not periodic arrays). The time-harmonic and time-dependent radiation produced by deterministic fractal arrays in the form of Paskal-Sierpinski gaskets was first studied by Lakhtakia et al. [74]. In particular, the radiation characteristics were examined for Paskal-Sierpinski arrays, comprised of Hertzian dipole sources located at each of the gasket nodes. A family of nonuniform arrays, known as Weierstrass arrays, was first introduced in [75]. These arrays have the property that their element spacings and current distributions are self-scalable and can be generated in a recursive fashion. Synthesis techniques for fractal radiation patterns were developed in [76, 77], based on the self-scalability property characteristic of discrete linear Weierstrass arrays, and the more general class of discrete linear Fourier-Weierstrass arrays. A fractal radiation-pattern synthesis technique for continuous line sources was also presented in [76]. The synthesis techniques developed for linear Weierstrass arrays were later extended to include concentric-ring arrays by Liang et al. [78].

5.2 Multi-Band Fractal Arrays

A design methodology for multi-band Weierstrass fractal arrays was introduced in [79, 80]. The application of fractal concepts to the design of multi-band Koch arrays, as well as multi-band and low-sidelobe Cantor arrays, were discussed in [81, 54]. A simplified Koch multi-band array, using windowing and quantization techniques, was presented in [82]. Finally, it was recently shown, in [83-85], that the Weierstrass-type and the Koch-type of multi-band arrays, previously considered independently in [79, 80] and [81, 54], respectively, are actually special cases of a more general unified family of self-scalable multi-band arrays. A contour plot of the far-field radiation pattern produced by a multi-band Weierstrass planar array is included in Figure 17.

5.3 Cantor, Sierpinski Carpet, and Related Arrays

Other properties of Cantor fractal linear arrays have been studied more recently in [10, 86, 87]. The radiation characteristics of planar concentric-ring Cantor arrays were investigated in [88-90]. These arrays were constructed using polyadic Cantor bars, which are described by their similarity fractal dimension, number of gaps, and lacunarity parameter. Planar fractal array configurations, based on Sierpinski carpets, were also considered in [10, 86, 87]. The fact that Sierpinski carpet and related arrays can be gen-

erated recursively (i.e., via successive stages of growth starting from a simple generating array) has been exploited in order to develop rapid algorithms for use in efficient radiation-pattern computations and adaptive beamforming, especially for arrays with multiple stages of growth that contain a relatively large number of elements [10, 11, 91, 92]. An example of a thinned hexagonal array, formed by this recursive procedure, is shown in Figure 18. The generating sub-array in this case is the hexagonal array depicted in the upper-right-hand corner of Figure 18. The array elements are located at the vertices of the hexagon. The first four stages of growth are indicated by the blue (Stage 1), red (Stage 2), green (Stage 3), and orange (Stage 4) arrays, respectively. Contour plots of the corresponding radiation patterns for each of these four arrays are illustrated in Figure 19. The Cantor linear and Sierpinski-carpet planar fractal arrays were also shown to be examples of deterministically thinned arrays [10, 86, 87]. An efficient recursive procedure was developed in [93] for calculating the driving-point impedance of linear and planar fractal arrays. For example, the first four stages in the growth of a triadic Cantor linear array of half-wave dipoles are shown in Figure 20. There are a total of $N_P = 2^P$ uniformly excited dipole elements at each stage of growth, P. Plots of the impedance matrix of the Cantor array for the first six stages of growth are presented in Figure 21. These illustrations clearly portray the self-similar fractal structure of the impedance matrix. Finally, a method for generating sum and difference patterns, which makes use of Sierpinski carpet fractal subarrays, was outlined in [94].

5.4 IFS Arrays and Compact Arrays

An iterated function system (IFS) approach for the design of fractal arrays was proposed by Baharav [95]. The use of IFS provides a very flexible design tool, which enables a wide variety of fractal array configurations, with many degrees of freedom, to be easily generated. A method for array sidelobe reduction by small position offsets of fractal elements was investigated in [96]. It was shown that because of their compact size and reduced coupling, the use of fractal antenna elements allows more freedom to accommodate position adjustments in phased arrays, which can lead to a suppression of undesirable sidelobes or grating lobes. The advantages of reduced mutual coupling and tighter packing, which can be achieved by using fractal elements in otherwise conventional
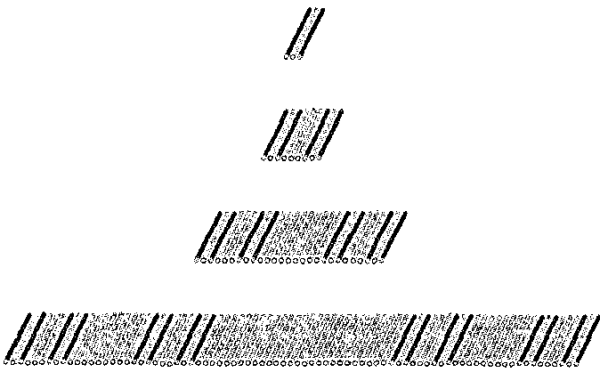

Figure 20. The first four stages in the process of generating a triadic Cantor linear array of half-wave dipoles. The dark gray dipoles represent physical elements, while the light gray dipoles are virtual elements.
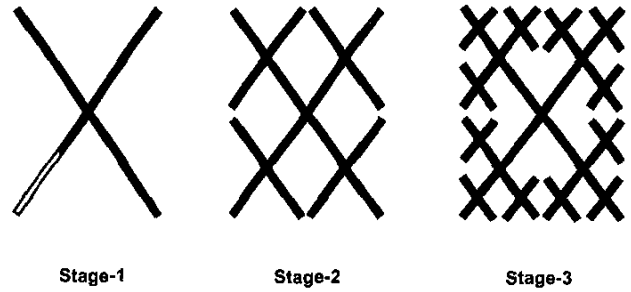

Figure 22. The design of a tri-band FSS using fractal elements: The first three stages in the construction of a crossbar fractal tree.

arrays, have also been investigated by Gianvittorio and Rahmat-Samii [97]. A genetic-algorithm approach for optimizing fractal dipole antenna arrays for compact size and improved driving-point impedance performance over scan angle was presented in [98]. The technique introduces fractal dipoles as array elements, and uses a genetic algorithm to optimize the shape of each individual fractal element (for self-impedance control), as well as the spacing between these elements (for mutual-impedance control). A useful method for interpolating the input impedance of fractal dipole antennas via a genetic-algorithm-trained neural network (called IFS-GA-NN) was presented in [99]. One of the main advantages of this IFS-GA-NN approach is that it is more computationally efficient than a direct Method of Moments analysis technique. For example, the method could be used in conjunction with genetic algorithms to more efficiently optimize arrays of fractal dipole elements, such as those considered in [98].

5.5 Diffraction from Fractal Screens and Apertures

Lakhtakia et al. [100] demonstrated that the diffracted field of a self-similar fractal screen also exhibits self-similarity. This finding was based on results obtained using a particular example of a fractal screen constructed from a Sierpinski carpet. Diffraction from Sierpinski carpet apertures has also been considered in [9], [11], [101], and [102]. The related problems of diffraction by fractally serrated apertures and Cantor targets have been investigated in [103-111].

6. Fractal Frequency-Selective Surfaces

Fractals were originally proposed for use in the design of frequency-selective surfaces (FSSes) by Parker and Sheikh [112]. This application makes use of the space-filling properties of certain fractals, such as the Minkowski loop and the Hilbert curve, in order to reduce the overall size of the unit cells that constitute an FSS. A dual-band fractal FSS design, based on a two-iteration Sierpinski gasket dipole, was first demonstrated in [113-115]. It was shown that the fractal FSS reported in [113-115] exhibits two stop-bands with attenuation in excess of 30 dB. Another possible approach that uses fractal tree configurations for realizing multiband FSS designs was first suggested in [42]. A particular example was considered by Werner and Lee [116, 117], where a tri-band FSS was designed using Stage 3 crossbar fractal tree elements. The first three stages in the construction of a crossbar fractal tree are illustrated in Figure 22. Figure 23 shows four adjacent cells of a

tri-band FSS. In this case, the individual elements or cells of this FSS are made up of Stage 3 crossbar fractal trees, which provide the required tri-band behavior. The transmission coefficient as a function of frequency is plotted in Figure 23 for a Stage 1, Stage 2, and Stage 3 crossbar fractal FSS. The stop-band attenuations of this fractal FSS were found to be in the neighborhood of 30 dB. This particular fractal FSS design approach also has the advantage of yielding the same response to either TE- or TM-mode excitation. Another noteworthy feature of this design technique is that the separation of bands can be controlled by choosing the appropriate scaling used in the fractal crossbar screen elements. More recently, various other self-similar geometries have been explored for their potential use in the design of dual-band and dual-polarized FSSes [118].

7. Bent-Wire Antennas

There has been some recent work to suggest that some random fractal or non-fractal bent-wire antennas may, in some cases, offer performance improvements compared to wires that have strictly deterministic fractal geometries. For instance, a comparison of the radiation characteristics of deterministic fractal and non-fractal (or random fractal) loop antennas was made in [119]. From this comparison, it was concluded that while the loop geometry is one factor in determining the antenna performance, it is not as significant as its overall physical area and total wire length in the loop. In [120], the performance of Koch fractal and other bent-wire monopoles as electrically small antennas was analyzed and compared. It was found that the simpler, less compressed bent-wire geometries of the meander line and normal-mode helix exhibit similar or improved performance when compared to that of a Koch fractal monopole. Finally, a methodology has been developed in [121] that employs a genetic algorithm to evolve a class of miniature multi-band antennas, called stochastic antennas, which offer optimal performance characteristics. This method is more general than the approach outlined in [68, 69], since it is not restricted to fractal geometries, and there are no reactive loads required to achieve the desired multi-band performance. The main disadvantage of the method is the fact that the optimization procedure is much less efficient than the genetic-algorithm approach based on fractal antenna geometries generated via an IFS.

8. Conclusions

Applications of fractal geometry are becoming increasingly widespread in the fields of science and engineering. This article presented a comprehensive overview of the research area we call fractal antenna engineering. Included among the topics considered were 1.) design methodologies for fractal antenna elements, 2.) application of fractals to the design of antenna arrays, and 3.) frequency-selective surfaces with fractal screen elements. The field of fractal antenna engineering is still in the relatively early stages of development, with the anticipation of many more innovative advancements to come over the months and years ahead.

9. Acknowledgements

10. References

1. K. Fujimoto, A. Henderson, K. Hirasawa, and J. R. James, *Small Antennas*. New York, John Wiley & Sons, Research Studies Press, 1987.

2. A. K. Skrivervik, J.-F. Zurcher, O. Staub, and J. R. Mosig, "PCS Antenna Design: The Challenge of Miniaturization," *IEEE Antennas and Propagation Magazine*, 43, 4, August 2001, pp. 12-26.

3. S. Maci and G. Biffi Gentili, "Dual-Frequency Patch Antennas," *IEEE Antennas and Propagation Magazine*, 39, 6, Dec. 1997, pp. 13-20.

4. B. B. Mandelbrot, *The Fractal Geometry of Nature*, New York, W. H. Freeman, 1983.

5. D. L. Jaggard, "On Fractal Electrodynamics," in H. N. Kritikos and D. L. Jaggard (eds.), *Recent Advances in Electromagnetic Theory*, New York, Springer-Verlag, 1990, pp. 183-224.

6. D. L. Jaggard, "Fractal Electrodynamics and Modeling," in H. L. Bertoni and L. B. Felson (eds.), *Directions in Electromagnetic Wave Modeling*, New York, Plenum Publishing Co., 1991, pp. 435-446.

7. D. L. Jaggard, "Fractal Electrodynamics: Wave Interactions with Discretely Self-Similar Structures," in C. Baum and H. Kritikos (eds.), *Electromagnetic Symmetry*, Washington DC, Taylor and Francis Publishers, 1995, pp. 231-281.

8. D. H. Werner, "An Overview of Fractal Electrodynamics Research," *Proceedings of the 11th Annual Review of Progress in Applied Computational Electromagnetics (ACES) Volume II*, Naval Postgraduate School, Monterey, CA, March 1995, pp. 964-969.

9. D. L. Jaggard, "Fractal Electrodynamics: From Super Antennas to Superlattices," in J. L. Vehel, E. Lutton, and C. Tricot (eds.), *Fractals in Engineering*, New York, Springer-Verlag, 1997, pp. 204-221.

10. D. H. Werner, R. L. Haupt, and P. L. Werner, "Fractal Antenna Engineering: The Theory and Design of Fractal Antenna Arrays," *IEEE Antennas and Propagation Magazine*, 41, 5, October 1999, pp. 37-59.

11. D. H. Werner and R. Mittra (eds.), *Frontiers in Electromagnetics*, Piscataway, NJ, IEEE Press, 2000.

12. H. O. Peitgen, H. Jurgens, and D. Saupe, *Chaos and Fractals: New Frontiers of Science*, New York, Springer-Verlag, Inc., 1992.

13. M. F. Barnsley, *Fractals Everywhere, Second Edition*, New York, Academic Press Professional, 1993.

14. D. H. Werner, "Fractal Radiators," *Proceedings of the 4th Annual 1994 IEEE Mohawk Valley Section Dual-Use Technologies & Applications Conference, Volume I*, SUNY Institute of Technology at Utica/Rome, New York, May 23-26, 1994, pp. 478-482.

15. D. H. Werner, "Fractal Electrodynamics," invited seminar for the Central Pennsylvania Section of the IEEE, Bucknell University, Lewisburg, Pennsylvania, November 18, 1993.

16. N. Cohen, "Fractal Antennas: Part 1," *Communications Quarterly*, Summer, 1995, pp. 7-22.

17. N. Cohen and R. G. Hohlfeld, "Fractal Loops and the Small Loop Approximation," *Communications Quarterly*, Winter, 1996, pp. 77-81.

18. N. Cohen, "Fractal and Shaped Dipoles," *Communications Quarterly*, Spring, 1996, pp. 25-36.

19. N. Cohen, "Fractal Antennas: Part 2," *Communications Quarterly*, Summer, 1996, pp. 53-66.

20. C. Puente, J. Romeu, R. Pous, J. Ramis, and A. Hijazo, "Small but Long Koch Fractal Monopole," *IEE Electronics Letters*, 34, 1, January 1998, pp. 9-10.

21. C. P. Baliarda, J. Romeu, and A. Cardama, "The Koch Monopole: A Small Fractal Antenna," *IEEE Transactions on Antennas and Propagation*, AP-48, 11, November 2000, pp. 1773-1781.

22. P. Tang, "Scaling Property of the Koch Fractal Dipole," IEEE International Symposium on Antennas and Propagation *Digest, Volume 3*, Boston, Massachusetts, July 2000, pp. 150-153.

23. N. Cohen, "NEC2 Modeling of Fractal-Element Antennas (FES's)," *13th Annual Review of Progress in Applied Computational Electromagnetics (ACES), Volume I*, Naval Postgraduate School, Monterey, CA, March 1997, pp. 297-304.

24. N. Cohen, "Fractal Antenna Applications in Wireless Telecommunications," *Proceedings of the Electronics Industries Forum of New England*, 1997, pp. 43-49.

25. N. Cohen, "Are Fractals Naturally Frequency Invariant/Independent?," *15th Annual Review of Progress in Applied Computational Electromagnetics (ACES), Volume I*, Naval Postgraduate School, Monterey, CA, March 1999, pp. 101-106.

26. R. G. Hohlfeld and N. Cohen, "Self-Similarity and the Geometric Requirements for Frequency Independence in Antennae," *Fractals*, 7, 1, March 1999, pp. 79-84.

27. C. Puente, J. Romeu, R. Pous, X. Garcia, and F. Benitez, "Fractal Multiband Antenna Based on the Sierpinski Gasket," *IEE Electronics Letters*, 32, 1, January 1996, pp. 1-2.

28. C. Puente, J. Romeu, R. Pous, and A. Cardama, "On the Behavior of the Sierpinski Multiband Fractal Antenna," *IEEE Transactions on Antennas and Propagation*, AP-46, 4, April 1998, pp. 517-524.

29. C. Puente, J. Romeu, R. Bartoleme, and R. Pous, "Perturbation of the Sierpinski Antenna to Allocate Operating Bands," *IEE Electronics Letters*, 32, 24, November, 1996, pp. 2186-2188.

30. J. Callejon, A. R. Bretones, and R. Gomez Martin, "On the Application of Parametric Models to the Transient Analysis of Resonant and Multiband Antennas," *IEEE Transactions on Antennas and Propagation*, AP-46, 3, March 1998, pp. 312-317.

31. C. Puente, M. Navarro, J. Romeu, and R. Pous, "Variations on the Fractal Sierpinski Antenna Flare Angle," IEEE International Symposium on Antennas and Propagation *Digest, Volume 4*, Atlanta, Georgia, June 1998, pp. 2340-2343.

32. C. T. P. Song, P. S. Hall, H. Ghafouri-Shiraz, and D. Wake, "Sierpinski Monopole Antenna with Controlled Band Spacing and Input Impedance," *IEE Electronics Letters*, 35, 13, June 1999, pp. 1036-1037.

33. C. Borja, C. Puente, and A. Median, "Iterative Network Model to Predict the Behavior of a Sierpinski Fractal Network," *IEE Electronics Letters*, 34, 15, July 1998, pp. 1443-1445.

34. C. Puente, C. B. Borau, M. N. Rodero, and J. R. Robert, "An Iterative Model for Fractal Antennas: Application to the Sierpinski Gasket Antenna," *IEEE Transactions on Antennas and Propagation*, AP-48, 5, May 2000, pp. 713-719.

35. C. Puente and J. Soler, "Analysis of Fractal-Shaped Antennas Using the Multiperiodic Traveling Wave Vee Model," *Proceedings of the IEEE Antennas and Propagation Society International Symposium*, 3, Boston, Massachusetts, July 2001, pp. 158-161.

36. M. Navarro, J. M. Gonzalez, C. Puente, J. Romeu, and A. Aguasca, "Self-Similar Surface Current Distribution on Fractal Sierpinski Antenna Verified with Infra-Red Thermograms," IEEE International Symposium on Antennas and Propagation *Digest, Volume 3*, Orlando, Florida, July 1999, pp. 1566-1569.

37. J. M. Gonzalez, M. Navarro, C. Puente, J. Romeu, and A. Aguasca, "Active Zone Self-Similarity of Fractal-Sierpinski Antenna Verified Using Infra-Red Thermograms," *IEE Electronics Letters*, 35, 17, August 1999, pp. 1393-1394.

38. R. Breden and R. J. Langley, "Printed Fractal Antennas," *Proceeding of the IEE National Conference on Antennas and Propagation*, 1999, pp. 1-4.

39. L. Xu and M. Y. W. Chia, "Multiband Characteristics of Two Fractal Antennas," *Microwave and Optical Technology Letters*, 23, 4, Nov. 1999, pp. 242-245.

40. C. Puente, J. Claret, F. Sagues, J. Romeu, M. Q. Lopez-Salvans, and R. Pous, "Multiband Properties of a Fractal Tree Antenna Generated By Electrochemical Deposition," *IEE Electronics Letters*, 32, 25, December 1996, pp. 2298-2299.

41. M. Sindou, G. Ablart, and C. Sourdois, "Multiband and Wideband Properties of Printed Fractal Branched Antennas," *IEE Electronics Letters*, 35, 3, Feb. 1999, pp. 181-182.

42. D. H. Werner, A. R. Bretones, and B. R. Long, "Radiation Characteristics of Thin-wire Ternary Fractal Trees," *IEE Electronics Letters*, 35, 8, April 1999, pp. 609-610.

43. J. P. Gianvittorio and Y. Rahmat-Samii, "Fractal Element Antennas: A Compilation of Configurations with Novel Charac-

teristics," IEEE International Symposium on Antennas and Propagation *Digest, Volume 3*, Salt Lake City, Utah, July 2000, pp. 1688-1691.

44. J. Gianvittorio, *Fractal Antennas: Design, Characterization, and Applications*, PhD Dissertation, Department of Electrical Engineering, University of California Los Angeles, 2000.

45. J. S. Petko and D. H. Werner, "Dense 3-D Fractal Tree Structures as Miniature End-loaded Dipole Antennas," IEEE International Symposium on Antennas and Propagation *Digest, Volume 4*, San Antonio, Texas, June 2002, pp. 94-97.

46. G. J. Walker and J. R. James, "Fractal Volume Antennas," *IEE Electronics Letters*, **34**, 16, August 1998, pp. 1536-1537.

47. C. T. P. Song, P. S. Hall, H. Ghafouri-Shiraz, and D. Wake, "Fractal Stacked Monopole with Very Wide Bandwidth," *IEE Electronics Letters*, **35**, 12, June 1999, pp. 945-946.

48. E. S. Siah, B. L. Ooi, P. S. Kooi, and X. D. Xhou, "Experimental Investigation of Several Novel Fractal Antennas – Variants of the Sierpinski Gasket and Introducing Fractal FSS Screens," *Proceedings of the Asia Pacific Microwave Conference, Volume 1*, 1999, pp. 170-173.

49. J. Anguera, C. Puente, C. Borja, and J. Romeu, "Miniature Wideband Stacked Microstrip Patch Antenna Based on the Sierpinski Fractal Geometry," IEEE International Symposium on Antennas and Propagation *Digest, Volume 3*, Salt Lake City, Utah, July 2000, pp. 1700-1703.

50. C. Puente, "Fractal-Shaped Antennas and Their Application to GSM 900/1800," *Proceedings of the Millennium Conference on Antennas and Propagation*, Davos, Switzerland, April 2000.

51. J. Soler and J. Romeu, "Dual-Band Sierpinski Fractal Monopole Antenna," IEEE International Symposium on Antennas and Propagation *Digest, Volume 3*, Salt Lake City, Utah, July 2000, pp. 1712-1715.

52. J. S. Castany, J. R. Robert, and C. Puente, "Mod-P Sierpinski Fractal Multiband Antenna," *Proceedings of the Millennium Conference on Antennas and Propagation*, Davos, Switzerland, April 2000.

53. C. T. P. Song, P. S. Hall, H. Ghafouri-Shiraz, and I. Henning, "Shorted Fractal Sierpinski Monopole Antenna," IEEE International Symposium on Antennas and Propagation *Digest, Volume 3*, Boston, Massachusetts, July 2001, pp. 138-141.

54. C. Puente, "Fractal Antennas," PhD Dissertation, Department of Signal Theory and Communications, Universitat Politècnica de Catalunya, June, 1997.

55. D. H. Werner and J. Yeo, "A Novel Design Approach for Small Dual-Band Sierpinski Gasket Monopole Antennas," IEEE International Symposium on Antennas and Propagation *Digest, Volume 3*, Boston, Massachusetts, July 2001, pp. 632-635.

56. K. J. Vinoy, K. A. Jose, V. K. Varadan, and V. V. Varadan, "Resonant Frequency of Hilbert Curve Fractal Antennas," IEEE International Symposium on Antennas and Propagation *Digest, Volume 3*, Boston, Massachusetts, July 2001, pp. 648-651.

57. J. Anguera, C. Puente, and J. Soler, "Miniature Monopole Antenna Based on the Fractal Hilbert Curve," IEEE International Symposium on Antennas and Propagation *Digest, Volume 4*, San Antonio, Texas, June 2002, pp. 546-549.

58. J. Zhu, A. Hoorfar, and N. Engheta "Feed-point Effects in Hilbert-Curve Antennas," IEEE International Symposium on Antennas and Propagation and USNC/URSI National Radio Science Meeting *URSI Digest*, San Antonio, Texas, June 2002, p. 373.

59. C. Borja and J. Romeu, "Multiband Sierpinski Fractal Patch Antenna," IEEE International Symposium on Antennas and Propagation *Digest, Volume 3*, Salt Lake City, Utah, July 2000, pp. 1708-1711.

60. J. Romeu, C. Borja, S. Blanch, and J. Girona, "High Directivity Modes in the Koch Island Fractal Patch Antenna," IEEE International Symposium on Antennas and Propagation *Digest, Volume 3*, Salt Lake City, Utah, July 2000, pp. 1696-1699.

61. C. Borja and J. Romeu, "Fraction Vibration Modes in the Sierpinski Microstrip Patch Antenna," IEEE International Symposium on Antennas and Propagation *Digest, Volume 3*, Boston, Massachusetts, July 2001, pp. 612-615.

62. J. Romeu, A. Aguasca, S. Blanch, and J. Girona, "Observation of Localized Modes in the Koch Waveguide," IEEE International Symposium on Antennas and Propagation *Digest, Volume 3*, Boston, Massachusetts, July 2001, pp. 644-647.

63. J. Yeo and R. Mittra, "Modified Sierpinski Gasket Patch Antenna for Multiband Applications," IEEE International Symposium on Antennas and Propagation *Digest, Volume 3*, Boston, Massachusetts, July 2001, pp. 134-137.

64. J. Anguera, C. Puente, C. Borja, and R. Montero, "Bowtie Microstrip Patch Antenna Based on the Sierpinski Fractal," IEEE International Symposium on Antennas and Propagation *Digest, Volume 3*, Boston, Massachusetts, July 2001, pp. 162-165.

65. J. Parron, J. M. Rius, and J. Romeu, "Analysis of a Sierpinski Fractal Patch Antenna Using the Concept of Macro Basis Functions," IEEE International Symposium on Antennas and Propagation *Digest, Volume 3*, Boston, Massachusetts, July 2001, pp. 616-619.

66. I. Kim, T. Yoo, J. Yook, and H. Park, "The Koch Island Fractal Microstrip Patch Antenna," IEEE International Symposium on Antennas and Propagation *Digest, Volume 2*, Boston, Massachusetts, July 2001, pp. 736-739.

67. J. Gianvittorio and Y. Rahmat-Samii, "Fractal Patch Antennas: Miniaturizing Resonant Patches," IEEE International Symposium on Antennas and Propagation and USNC/URSI National Radio Science Meeting *URSI Digest*, Boston, Massachusetts, July 2001, p. 298.

68. D. H. Werner, P. L. Werner, K. H. Church, J. W. Culver, and S. D. Eason, "Genetically Engineered Dual-Band Fractal Antennas," IEEE International Symposium on Antennas and Propagation *Digest, Volume 3*, Boston, Massachusetts, July 2001, pp. 628-631.

69. D. H. Werner, P. L. Werner, and K. H. Church, "Genetically Engineered Multi-Band Fractal Antennas," *IEE Electronics Letters*, **37**, 19, Sept. 2001, pp. 1150-1151.

70. S. D. Eason, R. Libonati, J. W. Culver, D. H. Werner, and P. L. Werner, "UHF Fractal Antennas," IEEE International Symposium on Antennas and Propagation *Digest, Volume 3*, Boston, Massachusetts, July 2001, pp. 636-639.

71. D. H. Werner, P. L. Werner, J. W. Culver, S. D. Eason, and R. Libonati, "Load Sensitivity Analysis for Genetically Engineered Miniature Multiband Fractal Dipole Antennas," IEEE International Symposium on Antennas and Propagation *Digest, Volume 4*, San Antonio, Texas, June 2002, pp. 86-89.

72. M. J. Wilhelm, D. H. Werner, P. L. Werner, K. Church, and R. Taylor, "Direct-Write Processes as Enabling Tools for Novel Antenna Development," IEEE International Symposium on Antennas and Propagation *Digest, Volume 4*, San Antonio, Texas, June 2002, pp. 102-105.

73. Y. Kim and D. L. Jaggard, "The Fractal Random Array," *Proc. IEEE*, 74, 9, 1986, pp. 1278-1280.

74. A. Lakhtakia, V. K. Varadan, and V. V. Varadan, "Time-harmonic and Time-dependent Radiation by Bifractal Dipole Arrays," *Int. J. Electronics*, 63, 6, 1987, pp. 819-824.

75. D. H. Werner and P. L. Werner, "Fractal Radiation Pattern Synthesis," USNC/URSI National Radio Science Meeting *Digest*, Boulder, Colorado, January 1992, p. 66.

76. D. H. Werner and P. L. Werner, "On the Synthesis of Fractal Radiation Patterns," *Radio Science*, 30, 1, January-February 1995, pp. 29-45.

77. P. L. Werner, D. H. Werner, and A. J. Ferraro, "Fractal Arrays and Fractal Radiation Patterns," *Proceedings of the 11th Annual Review of Progress in Applied Computational Electromagnetics (ACES), Volume II*, Naval Postgraduate School, Monterey, CA, March 1995, pp. 970-978.

78. X. Liang, W. Zhensen, and W. Wenbing, "Synthesis of Fractal Patterns From Concentric-Ring Arrays," *IEE Electronics Letters*, 32, 21, October 1996, pp. 1940-1941.

79. D. H. Werner and P. L. Werner, "Frequency-independent Features of Self-Similar Fractal Antennas," *Radio Science*, 31, 6, November-December 1996, pp. 1331-1343.

80. D. H. Werner, P. L. Werner, and A. J. Ferraro, "Frequency-Independent Features of Self-Similar Fractal Antennas," IEEE International Symposium on Antennas and Propagation *Digest, Volume 3*, Baltimore, Maryland, July 1996, pp. 2050-2053.

81. C. Puente Baliarda and R. Pous, "Fractal Design of Multiband and Low Side-lobe Arrays," *IEEE Transactions on Antennas and Propagation*, AP-44, 5, May 1996, pp. 730-739.

82. S. E. El-Khamy, M. A. Aboul-Dahab, and M. I. Elkashlan, "A Simplified Koch Multiband Fractal Array Using Windowing and Quantization Techniques," IEEE International Symposium on Antennas and Propagation *Digest, Volume 3*, Salt Lake City, Utah, July 2000, pp. 1716-1719.

83. D. H. Werner, M. A. Gingrich, and P. L. Werner, "A Generalized Fractal Radiation Pattern Synthesis Technique for the Design of Multiband and Broadband Arrays," IEEE International Symposium on Antennas and Propagation and USNC/URSI National Radio Science Meeting *URSI Digest*, Salt Lake City, Utah, July 2000, p. 281.

84. M. A. Gingrich, D. H. Werner, and P. L. Werner, "A Self-Similar Fractal Radiation Pattern Synthesis Technique for the Design of Multi-Band and Broad-Band Arrays," *Proceedings of the 17th Annual Review of Progress in Applied Computational Electromagnetics (ACES)*," Naval Postgraduate School, Monterey, CA, March 2001, pp. 53-60.

85. D. H. Werner, M. A. Gingrich, and P. L. Werner, "A Self-Similar Fractal Radiation Pattern Synthesis Technique for Reconfigurable Multi-Band Arrays," accepted for publication in the *IEEE Transactions on Antennas and Propagation*.

86. R. L. Haupt and D. H. Werner, "Fast Array Factor Calculations for Fractal Arrays," *Proceedings of the 13th Annual Review of Progress in Applied Computational Electromagnetics (ACES), Volume I*, Naval Postgraduate School, Monterey, CA, March 1997, pp. 291-296.

87. D. H. Werner and R. L. Haupt, "Fractal Constructions of Linear and Planar Arrays," IEEE International Symposium on Antennas and Propagation *Digest, Volume 3*, Montreal, Canada, July 1997, pp. 1968-1971.

88. D. L. Jaggard and A. D. Jaggard, "Cantor Ring Arrays," IEEE International Symposium on Antennas and Propagation *Digest, Volume 2*, Atlanta, Georgia, June 1998, pp. 866-869.

89. D. L. Jaggard and A. D. Jaggard, "Cantor Ring Arrays," *Microwave and Optical Technology Letters*, 19, 1998, pp. 121-125.

90. D. L. Jaggard and A. D. Jaggard, "Fractal Ring Arrays," invited paper submitted to *Wave Motion*, L. Felson and N. Engheta eds. of special issue, 1999.

91. D. H. Werner and P. L. Werner, "The Radiation Characteristics of Recursively Generated Self-Scalable and Self-Similar Arrays," *Proceedings of the 16th Annual Review of Progress in Applied Computational Electromagnetics (ACES), Volume II*, Naval Postgraduate School, Monterey, CA, March 2000, pp. 829-836.

92. D. H. Werner and P. L. Werner, "A General Class of Self-Scalable and Self-Similar Arrays," IEEE International Symposium on Antennas and Propagation *Digest, Volume 4*, Orlando, Florida, July 1999, pp. 2882-2885.

93. D. Baldacci and D. H. Werner, "An Efficient Recursive Procedure for Calculating the Driving Point Impedance of Linear and Planar Fractal Arrays," IEEE International Symposium on Antennas and Propagation *Digest, Volume 3*, Boston, Massachusetts, July 2001, pp. 620-623.

94. D. H. Werner, K. C. Anushko, and P. L. Werner, "The Generation of Sum and Difference Patterns Using Fractal Subarrays," *Microwave and Optical Technology Letters*, 22, 1, July 1999, pp. 54-57.

95. Z. Baharav, "Fractal Arrays Based on Iterated Function Systems (IFS)," IEEE International Symposium on Antennas and Propagation *Digest, Volume 4*, Orlando, Florida, July 1999, pp. 2686-2689.

96. N. Cohen and R. G. Hohlfeld, "Array Sidelobe Reduction by Small Position Offsets of Fractal Elements," *Proceedings of the 16th Annual Review of Progress in Applied Computational Electromagnetics (ACES), Volume II*, Naval Postgraduate School, Monterey, CA, March 2000, pp. 822-828.

97. J. P. Gianvittorio and Y. Rahmat-Samii, "Fractal Elements in Array Antennas: Investigating Reduced Mutual Coupling and Tighter Packing," IEEE International Symposium on Antennas and Propagation *Digest, Volume 3*, Salt Lake City, Utah, July 2000, pp. 1704-1707.

98. S. Mummareddy, D. H. Werner, and P. L. Werner, "Genetic Optimization of Fractal Dipole Antenna Arrays for Compact Size and Improved Impedance Performance Over Scan Angle," IEEE International Symposium on Antennas and Propagation *Digest, Volume 4*, San Antonio, Texas, June 2002, pp. 98-101.

99. K. M. Neiss, D. H. Werner, M. G. Bray, and S. Mummareddy, "Nature-Based Antenna Design: Interpolating the Input Impedance of Fractal Dipole Antennas via a Genetic Algorithm Trained Neural Network," IEEE International Symposium on Antennas and Propagation and USNC/URSI National Radio Science Meeting *URSI Digest*, San Antonio, Texas, June 2002, p. 374.

100. A. Lakhtakia, N. S. Holter, and V. K. Varadan, "Self-Similarity in Diffraction by a Self-similar Fractal Screen," *IEEE Transactions on Antennas and Propagation*, AP-35, 2, February 1987, pp. 236-239.

101. C. Allain and M. Cloitre, "Spatial Spectrum of a General Family of Self-similar Arrays," *Phys. Rev. A*, 36, 1987, pp. 5751-5757.

102. D. L. Jaggard and A. D. Jaggard, "Fractal Apertures: The Effect of Lacunarity," IEEE International Symposium on Antennas and Propagation and North American Radio Science Meeting *URSI Digest*, Montreal, Canada, July 1997, p. 728.

103. M. M. Beal and N. George, "Features in the Optical Transform of Serrated Apertures and Disks," *J. Opt. Soc. Am.*, A6, 1989, pp. 1815-1826.

104. Y. Kim, H. Grebel, and D. L. Jaggard, "Diffraction by Fractally Serrated Apertures," *J. Opt. Soc. Am.*, A8, 1991, pp. 20-26.

105. D. L. Jaggard, T. Spielman, and X. Sun, "Fractal Electrodynamics and Diffraction by Cantor Targets," IEEE International Symposium on Antennas and Propagation and North American Radio Science Meeting *URSI Digest*, London, Ontario, Canada, June 1991, p. 333.

106. T. Spielman and D. L. Jaggard, "Diffraction by Cantor Targets: Theory and Experiments," IEEE International Symposium on Antennas and Propagation and North American Radio Science Meeting *URSI Digest*, Chicago, Illinois, July 1992, p. 225.

107. D. L. Jaggard and T. Spielman, "Diffraction From Triadic Cantor Targets," *Microwave and Optical Technology Letters*, 5, 1992, pp. 460-466.

108. D. L. Jaggard, T. Spielman, and M. Dempsey, "Diffraction by Two-dimensional Cantor Apertures," IEEE International Symposium on Antennas and Propagation and USNC/URSI Radio Science Meeting *URSI Digest*, Ann Arbor, Michigan, June/July 1993, p. 314.

109. D. L. Jaggard and A. D. Jaggard, "Polyadic Cantor Superlattices with Variable Lacunarity," *Opt. Lett.*, 22, 1997, pp. 145-147.

110. A. D. Jaggard and D. L. Jaggard, "Cantor Ring Diffractals," *Optics Communications*, 158, 1998, pp. 141-148.

111. A. D. Jaggard and D. L. Jaggard, "Scattering from Fractal Superlattices with Variable Lacunarity," *J. Opt. Soc. Am. A*, 15, 1998, pp. 1626-1635.

112. E. A. Parker and A. N. A. El Sheikh, "Convoluted Array Elements and Reduced Size Unit Cells for Frequency-Selective Surfaces," *IEE Proceedings H*, 138, 1, Feb. 1991, pp. 19-22.

113. J. Romeu and Y. Rahmat-Samii, "A Fractal Based FSS with Dual Band Characteristics," IEEE International Symposium on Antennas and Propagation *Digest, Volume 3*, Orlando, Florida, July 1999, pp. 1734-1737.

114. J. Romeu and Y. Rahmat-Samii, "Dual Band FSS with Fractal Elements," *IEE Electronics Letters*, 35, 9, April 1999, pp. 702-703.

115. J. Romeu and Y. Rahmat-Samii, "Fractal FSS: A Novel Dual-Band Frequency Selective Surface," *IEEE Transactions on Antennas and Propagation*, 48, 7, July 2000, pp. 1097-1105.

116. D. H. Werner and D. Lee, "A Design Approach for Dual-Polarized Multiband Frequency Selective Surfaces Using Fractal Elements," IEEE International Symposium on Antennas and Propagation *Digest, Volume 3*, Salt Lake City, Utah, July 2000, pp. 1692-1695.

117. D. H. Werner and D. Lee, "Design of Dual-Polarized Multiband Frequency Selective Surfaces Using Fractal Elements," *IEE Electronics Letters*, 36, 6, March 2000, pp. 487-488.

118. J. P. Gianvittorio, Y. Rahmat-Samii, and J. Romeu, "Fractal FSS: Various Self-Similar Geometries Used for Dual-Band and Dual-Polarized FSS," IEEE International Symposium on Antennas and Propagation *Digest, Volume 3*, Boston, Massachusetts, July 2001, pp. 640-643.

119. S. R. Best, "The Fractal Loop Antenna: A Comparison of Fractal and Non-Fractal Geometries," IEEE International Symposium on Antennas and Propagation *Digest, Volume 3*, Boston, Massachusetts, July 2001, pp. 146-149.

120. S. R. Best, "On the Performance of the Koch Fractal and Other Bent Wire Monopoles as Electrically Small Antennas," IEEE International Symposium on Antennas and Propagation *Digest, Volume 4*, San Antonio, Texas, June 2002, pp. 534-537.

121. P. L. Werner and D. H. Werner, "A Design Optimization Methodology for Multiband Stochastic Antennas," IEEE International Symposium on Antennas and Propagation *Digest, Volume 2*, San Antonio, Texas, June 2002, pp. 354-357.

Introducing the Feature Article Author

Dr. Douglas H. Werner is an Associate Professor in the Pennsylvania State University Department of Electrical Engineering. He is a member of the Communications and Space Sciences Lab (CSSL), and is affiliated with the Electromagnetic Communication Research Lab. He is also a Senior Research Associate in the Electromagnetics and Environmental Effects Department of the Applied Research Laboratory at Penn State. Dr. Werner received the BS, MS, and PhD degrees in Electrical Engineering from the Pennsylvania State University in 1983, 1985, and 1989, respectively. He also received the MA degree in Mathematics there in 1986. Dr. Werner was presented with the 1993 Applied Computational Electromagnetics Society (ACES) Best Paper Award, and was also the recipient of a 1993 International Union of Radio Science (URSI) Young Scientist Award. In 1994, Dr. Werner received the Pennsylvania State University Applied Research Laboratory Outstanding Publication Award. He has also received several Letters of Commendation from the Pennsylvania State University Department of Electrical Engineering for outstanding teaching and research. Dr. Werner is a former Associate Editor of *Radio Science*, an Editor of the *IEEE Antennas and Propagation Magazine*, a Senior Member of the Institute of Electrical and Electronics Engineers (IEEE), a member of the American Geophysical Union (AGU), USNC/URSI Commissions B and G, the Applied Computational Electromagnetics Society (ACES), Eta Kappa Nu, Tau Beta Pi, and Sigma Xi. He has published numerous technical papers and proceedings articles, and is the author of eight book chapters. He recently published a new book for IEEE Press, entitled *Frontiers in Electromagnetics*. He has also contributed a chapter for a Wiley Interscience book entitled *Electromagnetic Optimization by Genetic Algorithms*. He was the recipient of a College of Engineering PSES Outstanding Research Award and Outstanding Teaching Award in March, 2000, and March, 2002, respectively. He was also recently presented with an IEEE Central Pennsylvania Section Millennium Medal.

His research interests include theoretical and computational electromagnetics, with applications to antenna theory and design, microwaves, wireless and personal communication systems, electromagnetic wave interactions with complex meta-materials, fractal and knot electrodynamics, and genetic algorithms.

Dr. **Suman Ganguly** has been working in the areas of Radio Science, Radio Engineering, Electronics, Ionospheric and Plasma Physics for over 30 years. He graduated from Calcutta University, India, with a Masters in Physics and Electronics in 1962. He obtained his PhD from the same university in 1970, specializing in Ionospheric Physics. Since then, he has been working in a variety of disciplines and in different institutions. He worked at Lancaster University, UK, dealing with the ATS-6 satellite beacon project. He joined Arecibo Observatory, Puerto Rico, during 1976, and worked with the 1000-foot radar, probing the ionosphere. During 1979, he joined Rice University, where he continued his research on ionospheric and plasma sciences. He was actively involved in ionospheric modification using high-powered radio waves, and the first ULF generation in the ionosphere at Arecibo was reported by him. During 1986, he started a small R&D organization, Center for Remote Sensing, in Virginia, and has been active in numerous projects involving communication, navigation, signal processing, electromagnetics, instrumentation, space science, and other areas of radio engineering. Center For Remote Sensing (http://www.cfrsi.com) comprises several engineers, and has provided advanced technology development to most of the government agencies as well as private organizations. He has over 200 publications, and is a member of numerous professional organizations.